

This article was downloaded by: [Université de Strasbourg, SCD]

On: 23 October 2012, At: 02:20

Publisher: Taylor & Francis

Informa Ltd Registered in England and Wales Registered Number: 1072954 Registered office: Mortimer House, 37-41 Mortimer Street, London W1T 3JH, UK



International Journal of Crashworthiness

Publication details, including instructions for authors and subscription information:
<http://www.tandfonline.com/loi/tcrs20>

Development and validation of a coupled head-neck FEM - application to whiplash injury criteria investigation

F. Meyer^a, N. Bourdet^a, K. Gunzel^a & R. Willinger^a

^a University of Strasbourg, IMFS-CNRS, Strasbourg, France

Version of record first published: 23 Oct 2012.

To cite this article: F. Meyer, N. Bourdet, K. Gunzel & R. Willinger (2012): Development and validation of a coupled head-neck FEM - application to whiplash injury criteria investigation, International Journal of Crashworthiness, DOI:10.1080/13588265.2012.732293

To link to this article: <http://dx.doi.org/10.1080/13588265.2012.732293>



PLEASE SCROLL DOWN FOR ARTICLE

Full terms and conditions of use: <http://www.tandfonline.com/page/terms-and-conditions>

This article may be used for research, teaching, and private study purposes. Any substantial or systematic reproduction, redistribution, reselling, loan, sub-licensing, systematic supply, or distribution in any form to anyone is expressly forbidden.

The publisher does not give any warranty express or implied or make any representation that the contents will be complete or accurate or up to date. The accuracy of any instructions, formulae, and drug doses should be independently verified with primary sources. The publisher shall not be liable for any loss, actions, claims, proceedings, demand, or costs or damages whatsoever or howsoever caused arising directly or indirectly in connection with or arising out of the use of this material.

Development and validation of a coupled head-neck FEM – application to whiplash injury criteria investigation

F. Meyer*, N. Bourdet, K. Gunzel and R. Willinger

University of Strasbourg, IMFS-CNRS, Strasbourg, France

(Received 16 May 2012; final version received 18 September 2012)

The objective of the present study is to improve the understanding of whiplash injury mechanisms based on the extensive numerical simulation of real-world rear impact accidents with a detailed head–neck finite-element model (FEM). Based on an existing FE neck model and on an existing whiplash accident database including crash pulse recording, the present study proposes an in-depth investigation of the neck response at tissue level with the objective to extract pertinent ‘intra-cervical’ parameters presenting high correlation with the occurrence of whiplash injury.

Keywords: head-neck finite element model; whiplash injury; neck injury criteria

Introduction

Whiplash injury remains an acute road safety issue despite the huge effort developed over the last decade by the scientific community. Every year, whiplash injury costs \$ 4 billion in the USA, € 4 billion in Europe and € 2 billion in Japan. In the biomechanics field, we can underline, over the last decades, two major advances in the understanding of whiplash injury. The first concerns the experimental approach with the characterisation of the relative cervical vertebrae motion during a rear impact [28,34,48] and second the numerical tools based on finite-element (FE) modelling. Recent FE models are not just designed to predict head kinematics but are able to give insight into injury criteria in order to optimise different protection systems against intra-cervical parameters [22,35].

Before these recent advances, the injuries criteria were based on relative head and first thoracic vertebrae kinematics. Böstrom *et al.* [4] propose a criterion called Neck Injury Criterion (NIC), calculated from the relative acceleration and velocity between the head and the first thoracic vertebrae. It was rapidly adopted by the car industry because it expresses the relative motion between the head and T1 and it can be easily recorded on dummies with a high degree of repeatability. More recently, in 2002, Viano and Davidsson [42] proposed an injury criterion called Neck Displacement Criterion (NDC) based on the relative angular and linear displacement of the head and T1. Injury criteria based on a combination of the force and moment at the first thoracic vertebrae and at the atlanto occipital joint have also been proposed. The most frequently used criterion is the N_{km} [39] using the axial forces and the bending

moment at the head to neck junction. The N_{ij} criterion, established for the frontal impact, used a similar formulation but the force recorded (or computed) is in the vertical direction. Finally, the Lower Neck Load (LNL) injury criterion [21] refers to a combination of the moment and the force in the three directions at lower neck level.

If force- and moment-based criteria are well adapted to experimental investigation using dummies, this kind of criteria cannot be related to neck injury mechanisms. In order to progress towards tissue-level injury criteria, further medical and numerical investigations were undertaken in the early 2000 by a number of authors.

The first step for the characterisation of the cervical vertebrae motion during a rear impact was undertaken by Matsushita *et al.* [28], Yoganadan and Pinter [48] and Ono *et al.* [34]. However, Ono and Kaneoka [33] were the first to compare the cervical vertebrae motions, on living human, with physiological motions. One of their conclusions was that the a-physiological motions, commonly named ‘S-shaped’, induces a stretching of the cervical facet joint, previously described also by April and Bogduk [2] and Lord *et al.* [27]. Therefore, several authors, Winkelstein *et al.* [44], Deng *et al.* [14], Yoganandan *et al.* [50] and Sundararajan *et al.* [41], focused their work on the facet joint injury (zygapophysial joint pain) and concluded that whiplash neck injury is linked to this stretching. On the other hand, Panjabi *et al.* [36] realised five types of rear impact ranging from 2.5 to 10.5 g on Post Mortem Human Surrogate (PMHS) and did not find ‘strong correlation between the strain during the trauma and the sled acceleration’ according to these authors. The injury is located

*Corresponding author. Email: frmeier@unistra.fr

at the inter-vertebral disc which is respectively stretched and compressed in its anterior respectively posterior region. This result is in accordance with the study undertaken by Davis *et al.* [10] investigating nine patients after whiplash injuries through an MRI (magnetic resonance imaging) exam. It appeared that the patients had cervical disc herniations or ligament injuries. All the injuries were localised at the lower levels, i.e. C6-C7 or C5-C6. In 2005, Panjabi *et al.* proposed a new injury criterion called 'Inter-Vertebral Neck Injury Criterion (IV-NIC)' based on the hypothesis that inter-vertebral motion during the 'S-Shape' injures the spinal soft tissues. At each cervical level, the physiological limit was determined experimentally on fresh cadaver. The ratio of the dynamical angle and the physiological angle assesses the injury risk of the soft tissues (ligament, inter-vertebral disk, annulus fibre and facet joint) at each level. One of the major advances in the understanding of whiplash injuries concerns the accident database established by Kullgren *et al.* [25]. In this study, the authors reconstructed 79 real rear crash accidents with a multi-body model of Biorid dummy in order to evaluate the main injury criteria. The authors estimated that NIC and the N_{km} values were applicable to predict risk of neck AIS1 injury.

Concerning the FE aspect, in the last decades, a number of neck FE models were developed with different levels

of detail in terms of geometry, validation and mechanical properties. The main models were developed by De Jaeger *et al.* [12], Camacho *et al.* [7], Yang *et al.* [47], Halldin *et al.* [20], Lee *et al.* [26] and Meyer *et al.* [30]. These models were able to predict the head-neck kinematics but are not yet able to predict injury risk during a rear impact. The first study using a Neck FE Model (FEM) in order to offer a better protection was proposed by Kitagawa *et al.* [22] who conducted an optimisation of a car seat based on the relative displacement of the facet joint. Recently, Ono *et al.* [35] used the FE model developed by Ejima *et al.* [15] and Sugimoto and Yamazaki [40] and proposed a new injury criteria based on the strain rate of the facet joint. In this study, the model was validated in rear impact against human volunteer and cadaver experiments. Validation was provided in terms of maximal shear strain of the facet joint at each cervical level. For the first time, 20 real-world rear impacts were reconstructed by Ono *et al.* [35] in order to evaluate the classical injury parameter and to derive a threshold for the principal and shear strain of the facet joint. Good correlation was obtained for the facet strain and it appeared that the lower shear force can also be used to assess neck injury.

In this context, existing detailed head-neck FEMs are coupled in the present study and validated against recent experimental time and frequency responses of the head-neck

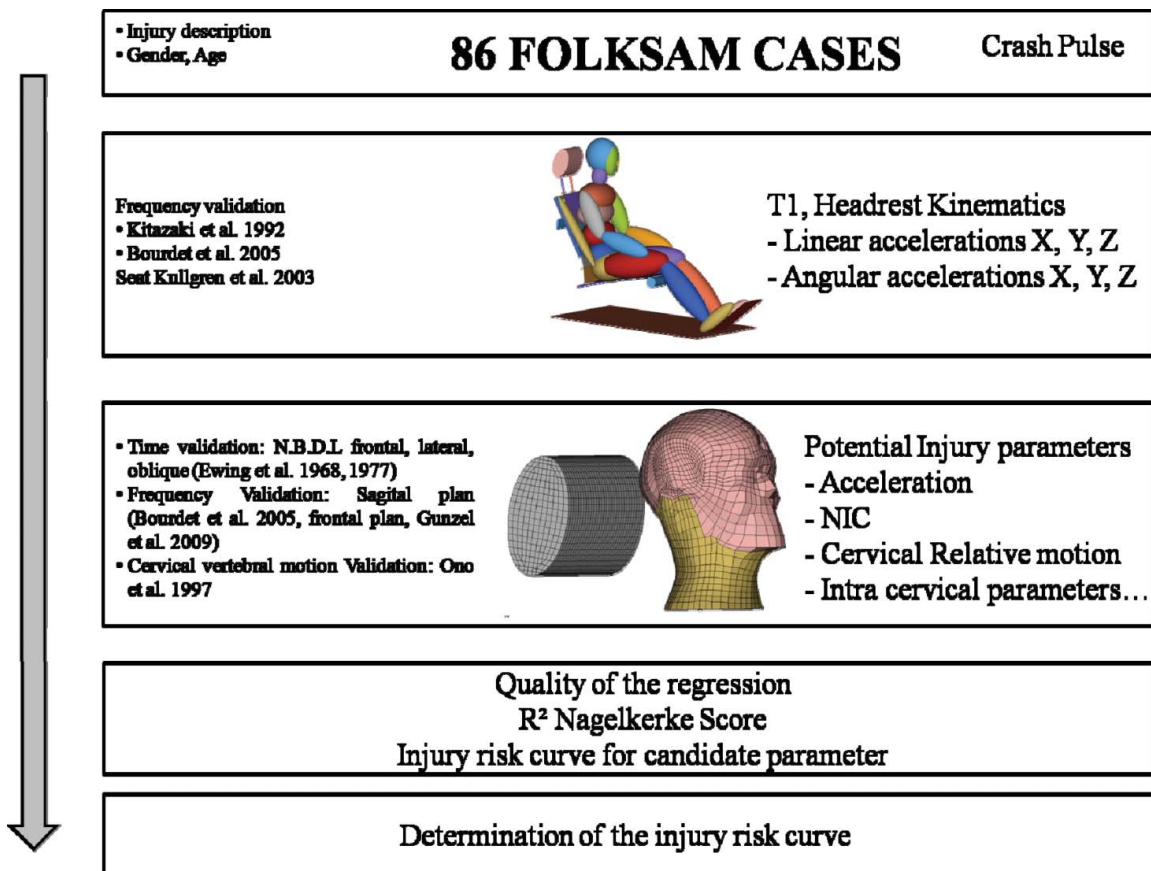


Figure 1. Methodology defined in order to determine neck tolerance limits in rear impact.

system. In a second step, the suggested methodology illustrated in Figure 1 considers the coupled head–neck FEM and a unique real-world whiplash accident database. For each accident case, the first thoracic vertebra acceleration has been computed based on a multi-body modelling of the seat and the human torso–head–neck complex and these 3D acceleration data were considered as the input of the FE simulation using the head–neck model. From this final simulation, a number of intra-cerebral and intra-cervical parameters are computed for each victim in order to conduct a correlation study between each mechanical parameter with the occurrence of neck pain sustained by the victim. For comparison purposes, existing injury parameters are computed as well and finally a statistical methodology based on a regressing analysis is applied to the results in order to derive the best candidate parameter for the discrimination of uninjured and injured cases, contributing those to the definition of neck injury mechanism understanding.

Material and methods

Rear-world accident database

In the present study, the crash pulse acceleration of 86 real-life rear-end impact from Folksam database have been reconstructed. The seat acceleration–time history was measured during the crash by a crash pulse recorder fixed on three car models of the same make. The recording and the analysis have been described by Aldman *et al.* [1] and Kullgren *et al.* [24,25]. The sampling rate of the crash pulse recorder is 1000 Hz during the impact phase of the crash and the recorded acceleration data were filtered at approximately 60 Hz.

The occupant injury severity was divided into four categories (Quebec classification of Whiplash-Associated disorder Table 1). Examples of symptoms are neck pain, headache, dizziness and neck stiffness. The numbers of victims are presented according to the various injury categories, car model and occupant location as well as the age and gender distribution in Table 2. It can be observed in this table that there is a similar proportion of males and females and ages distribution for occupants with symptoms over one month then for the total population.

Figure 2 shows that this database includes a large range of impact energy. The collected accidents present acceleration between 1 and 7 g and a delta V of 2 to 35 m/s.

Table 2. Gender and average age for occupants with various injury categories.

	Average age	Gender (%)		Number of cases
		Male	Female	
WAD0	46	52	48	57
WAD1	44	33	67	19
WAD2	48	40	60	5
WAD3	43	40	60	5
WAD4	–	–	–	0
Total	46	47	53	86

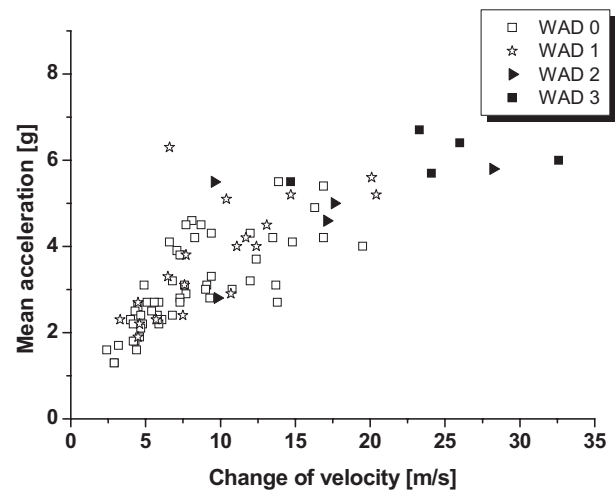


Figure 2. Relationship between change of velocity and mean acceleration.

Even if there is not a well-defined limit between uninjured and injured cases, it appears in Figure 2 that over 20 m/s (72 Km/h) and 5 g all the subjected involved sustained an injury. Otherwise for the low-intensity cases, injured and uninjured cases are represented.

This database includes only three types of cars, i.e. TOYOTA Corolla 93, Corolla 98 and Yaris. Kullgren *et al.* [25] modelised these three car seats. The mechanical properties of each seat were identified against experimental test using Biorid dummy and realised at an impact speed of 23 km/h and a mean acceleration of 4.5 g.

Table 1. Quebec classification of Whiplash-Associated Disorder (WAD).

Grade	Clinical classification
0	The neck has no symptoms, and the physical finding is normal.
1	The neck has pain and stiffness, but the physical finding is normal.
2	In addition to neck symptoms, there is a limit of motion space of the cervical vertebra and localised tender point, suggesting neck symptoms from musculoskeletal system.
3	In addition to neck symptoms, there are neurological findings such as the tendon reflex disorder, adynamia, and perception disorder.
4	Dislocation and fracture of the cervical vertebrae.

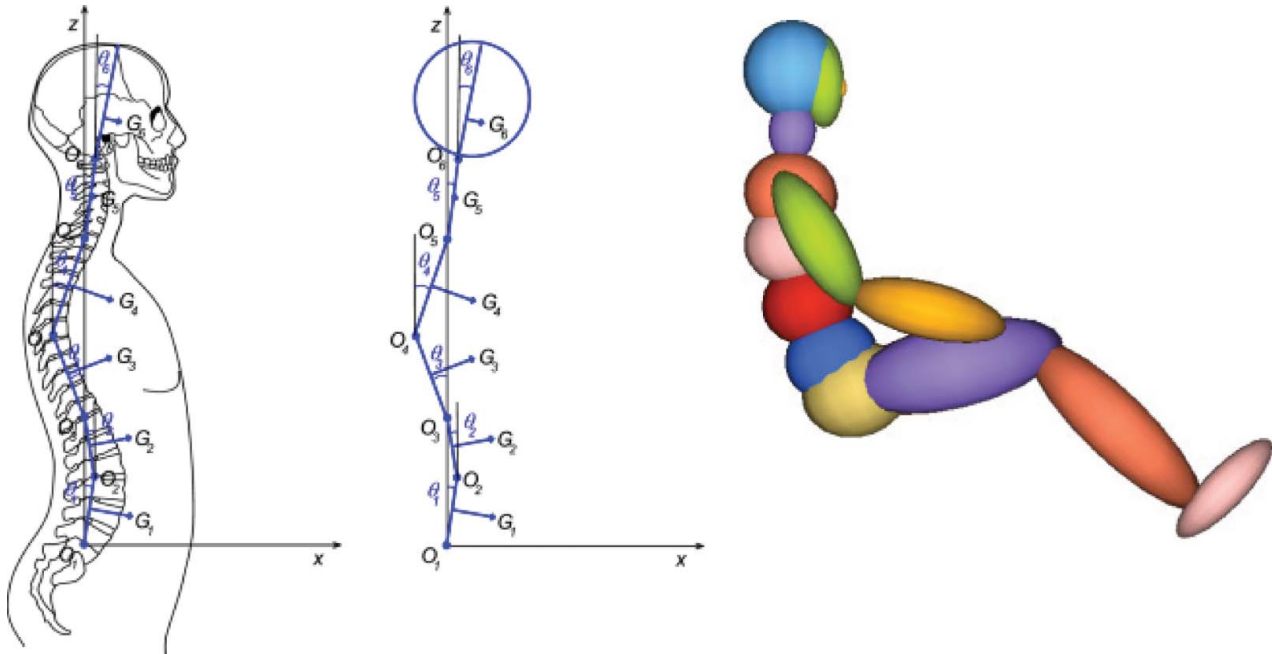


Figure 3. Representation of the lumped parameters model of the trunk.

Lumped torso model

A realistic lumped torso model is needed in order to determine the T1 3D kinematics for the 86 accident cases. In order to address this issue, an original lumped model of the human torso was developed. The hypothesis of linear behaviour was used as the torso is subjected to small deformations under rear impact. The modal analysis of the human torso in a seating position conducted by Kitazaki [23] was used for both masses and mechanical properties identification of the human thorax by Bourdet and Willinger [6].

In order to reproduce the four vibration mode shapes identified experimentally by Kitazaki [23], the torso was divided in six segments to obtain the five degrees of freedom including the head–neck system, as illustrated in Figure 3. This model is able to reproduce the four first experimental vibration modes and was validated in the frequency domain in terms of natural frequencies, damping and mode shapes. The method allowed it to identify the mechanical properties of the head–neck–torso model and to superimpose the numerical modal analysis with the experimental one as shown in Table 3.

Coupling of head–neck FEMs and validation

The head–neck model used in the present study is a coupling of two existing FEMs developed at the University of Strasbourg (UdS). This section presents the detailed model of the head–neck system and its validation against recent experimental data.

The head FEM considered in this study is the Strasbourg University FE Head Model (SUFEHM) presented in detail with its latest validation in Deck and Willinger [11] and illustrated in Figure 4. In total, the model is formed from 13,208 elements and has a mass of 4.7 Kg. Material properties implemented into the model are summarised in Appendix 1 and geometry is in accordance to [18].

A number of real-world head trauma simulations were conducted by these authors to provide head injury criteria for skull fracture, sub-dural haematoma and moderate or severe neurological injuries.

The Neck FEM considered in this study was published by Meyer *et al.* [30] and needed improvements in terms of meshing and mechanical properties in the framework of this coupling effort. The muscles originally represented by 58,179 bricks elements were reduced to 2691 in order to optimise the computation time. Moreover, spring

Table 3. Validation of the lumped torso model in terms on natural frequencies [6].

Mode shape	Experimental	
	[Hz]	Lumped-model [Hz]
1st mode head–neck (Flexion–extension)	1.6	1.4
2nd head–neck (S-shape)	8.8	8.8
1st mode thorax	1.82	1.9
2nd mode thorax	3.31	3.25
3rd mode thorax	6.16	6.2
4th mode thorax	17.58	17.2

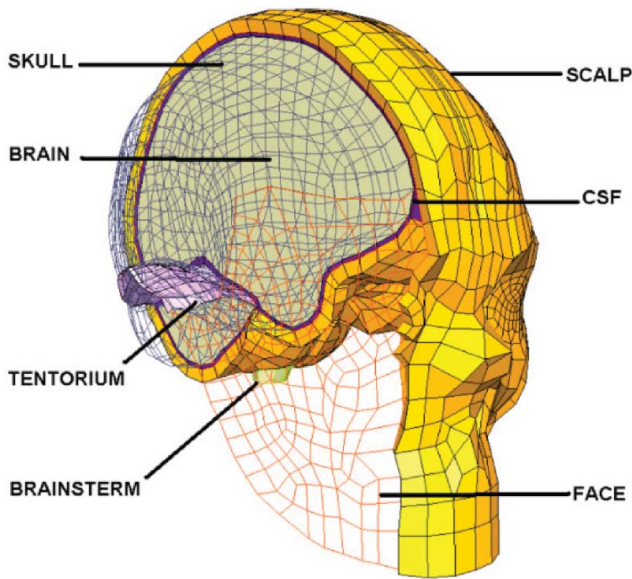


Figure 4. Cross section of the Strasbourg University Finite Element Head Model (SUFEHM).

elements were added to take into account muscles activation. The major muscles were included, i.e. Longissimus capitis; Longissimus cervicis; Longus capitis; Longus colli C1-C5; Longus colli C5-T1; Scanelus anterior; Scanelus medius; Scanelus posterior; Semispinalis capitis; Semispinalis cervicis; Splenius capitis; Splenius cervicis; Sternocleidomastoidien and the Trapezius.

To couple the head FEM to the neck FEM the face was completely remesh. The face previously modelised by shell elements was replaced by brick elements in order to have continuity between the face and the anterior muscles. More-

over, this type of element offers the possibility to obtain a realistic representation in terms of inertia.

Concerning the cervical spine, no modification was made in comparison to the previous neck FE. The cervical vertebrae are represented by shell elements, inter-vertebral disks by brick elements and the ligamentary systems by spring elements. Finally, the whole head-neck model is formed by 25,596 elements and has a mass of 6.5 Kg. A cross-section of the new head-neck FEM system is given in Figure 5.

The ligaments and the cervical vertebrae mechanical properties are similar to those reported in the previous study [30]. The main difference concerns the muscles which have a viscoelastic constitutive law for the brick elements and active hill law for the spring elements. Appendix 1 summarises the mechanical properties of the different head and neck anatomical parts. This coupling effort and model improvement obviously depend on a deep multidirectional time- and frequency-domain validation as well as a validation against vertebrae-relative motion.

Head-neck model validations

Due to the remeshing of the muscle parts and the coupling of the head FEM, it was necessary to validate the improved model against the NBDL tests in frontal, lateral and oblique impact situation according to Ewing *et al.* [16,17]. Results related to this time-domain validation are reported in Appendix 2 (Figures A1-A6). Further validation is then considered in the frequency domain by considering experimental modal analysis reported by Bourdet *et al.* [5] and Gunzel *et al.* [19].

Finally, this validation was completed by simulating the experience of Ono *et al.* [34] in order to evaluate the relative cervical motion under rear impact. It must be noticed that

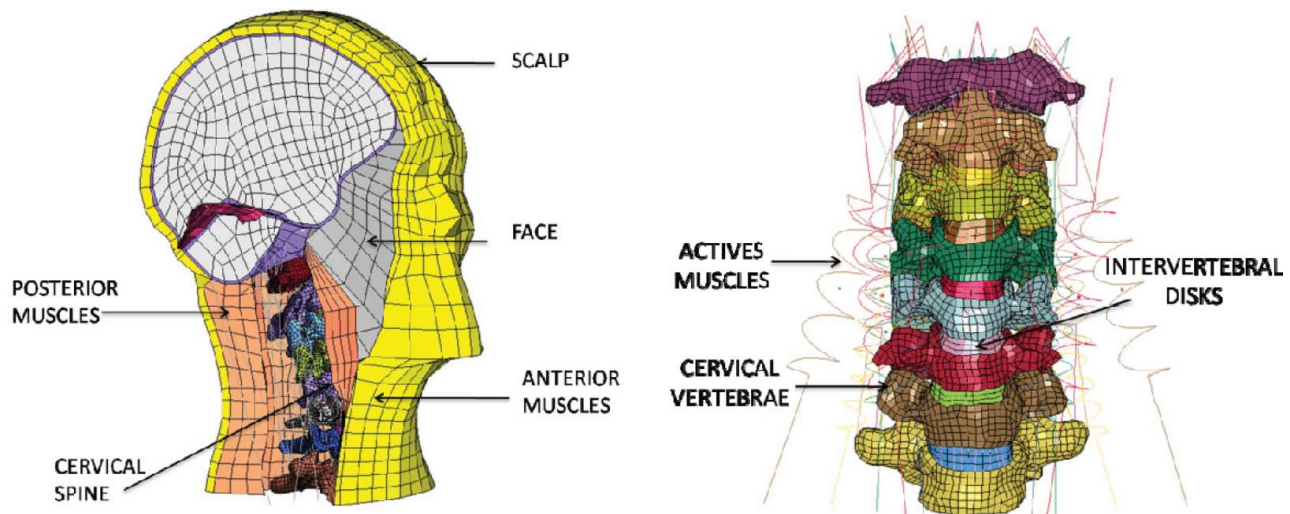


Figure 5. Cross section of the Strasbourg University human head-neck system FE model.

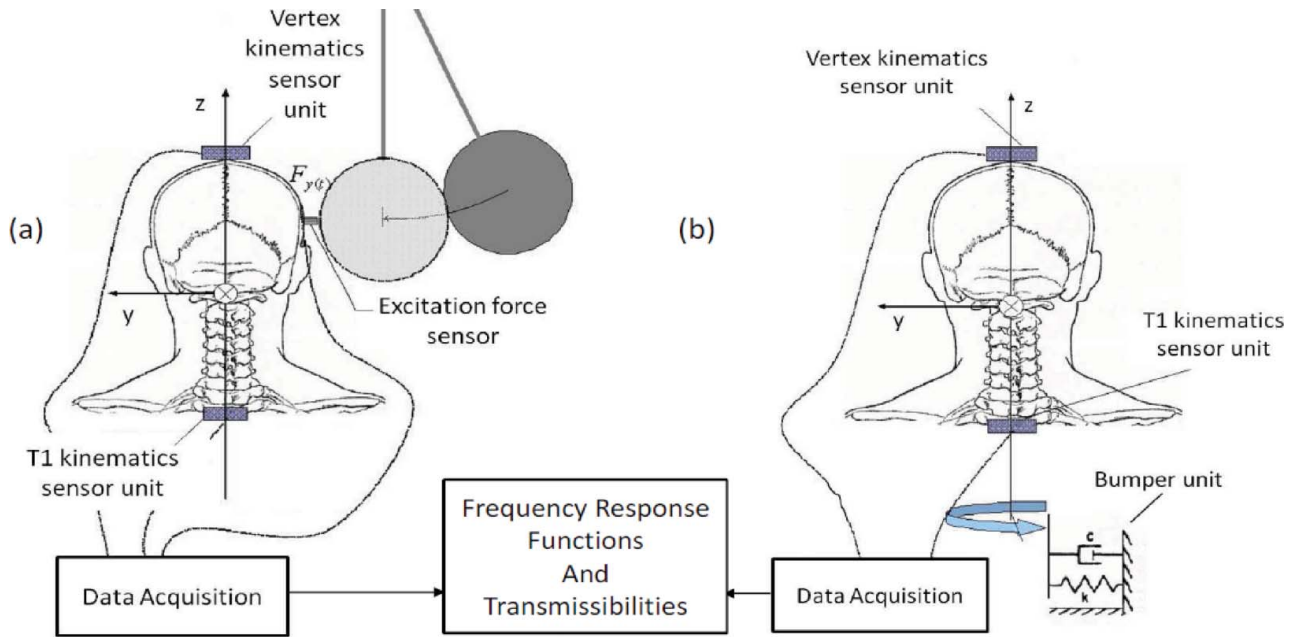


Figure 6. Experimental modal tests scheme under lateral (a) and rotational (b) simulation.

for the three different validations (NBDL, modal analysis and relative cervical vertebrae motion), the mechanical properties were exactly the same.

Multidirectional modal analysis

This section focuses on the validation of the FEM of the head/neck system in the frequency domain. In past studies, Bourdet *et al.* [5] and Meyer *et al.* [30] showed that a validation in the time domain is not sufficient to reproduce the dynamic behaviour of the neck. In fact, a great

amount of responses may exist in a given corridor. And these responses do not correspond to the same mechanical behaviour. More recently, Gunzel *et al.* [19] produced an extension of the head/neck system characterisation in the frontal and horizontal plane. Two kinds of experimental devices were therefore realised. The first one is the same as the one used by Bourdet *et al.* [5] and the second one consists of a rotational solicitation of the thorax (Figure 6). Ten volunteers were tested: six men and four women¹.

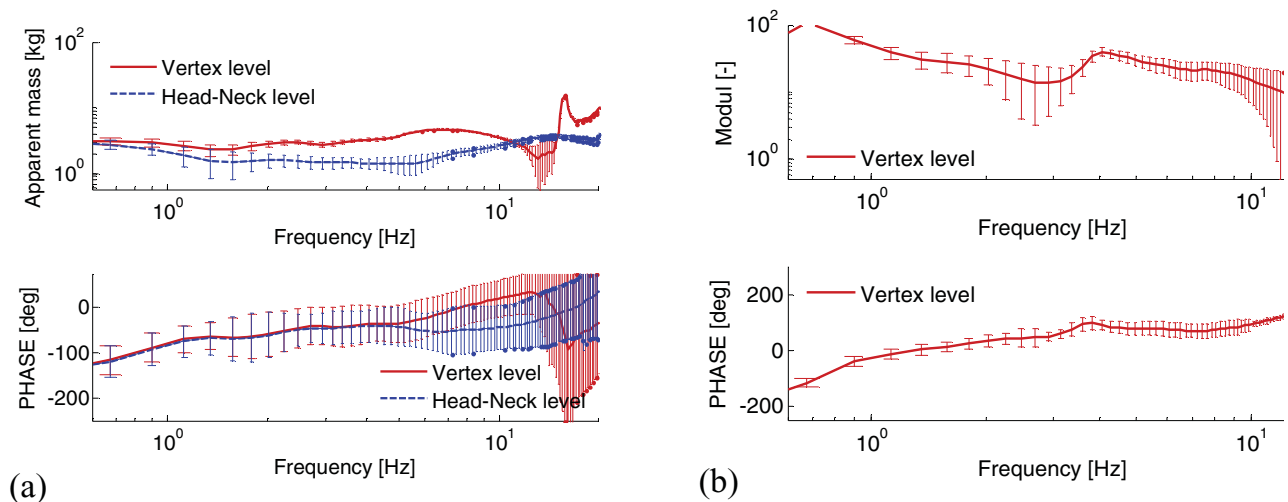


Figure 7. Averaged transfer functions estimated for the frontal plane for 10 volunteers. (a) transfer function between lateral excitation force and lateral acceleration of head and neck (b) transfer function between rotational excitation force.

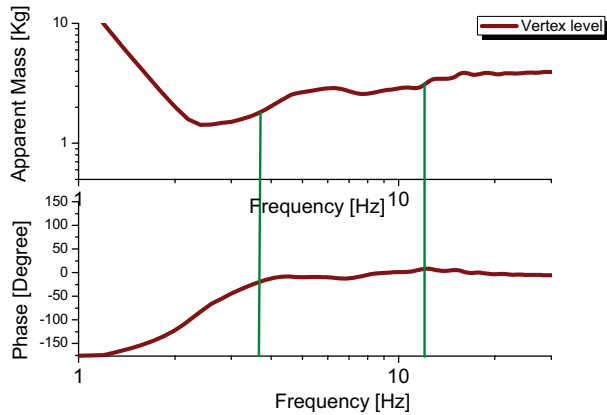


Figure 8. Transfer function in terms of apparent mass at head neck level in the sagittal plane.

Three resonance frequencies that correspond to three modal deforms were identified. The resonance frequencies were determined thanks to the calculation of the apparent mass and of the phase at the atlanto-occipital junction and at the vertex. The lateral solicitation tests allowed to identify a lateral inclination mode at 1.7 ± 0.2 Hz and a lateral retraction at 9.5 ± 1.4 Hz (Figure 7a). The third mode was identified thanks to the rotational tests which showed the rotational mode of the head at 3.2 ± 0.3 Hz (Figure 7b).

That modal characterisation in the frontal plane, coupled with the experimental tests in the same plane, allowed a multi-directional validation of the FEM of the head/neck system. The experimental tests in the sagittal and frontal planes, as well as around the axial direction, were reproduced numerically so as to identify the five vibration modes. The same output data as those which were recorded experimentally were calculated to be used in the same signal processing scheme. The results obtained thanks to the FEM of the head/neck system are illustrated in Figures 8–10 and summarised in Table 4.

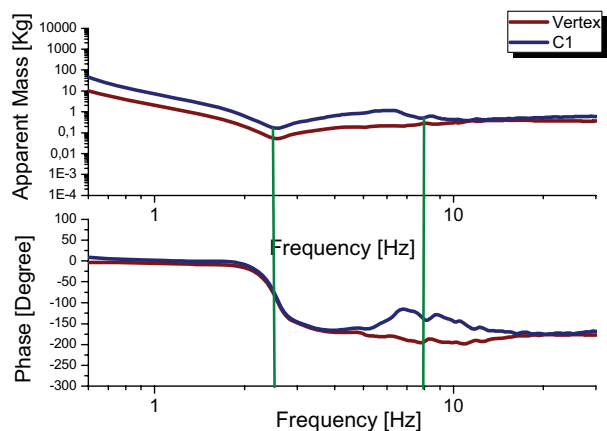


Figure 9. Transfer function in terms of apparent mass at head neck level in the frontal plane (lateral impact).

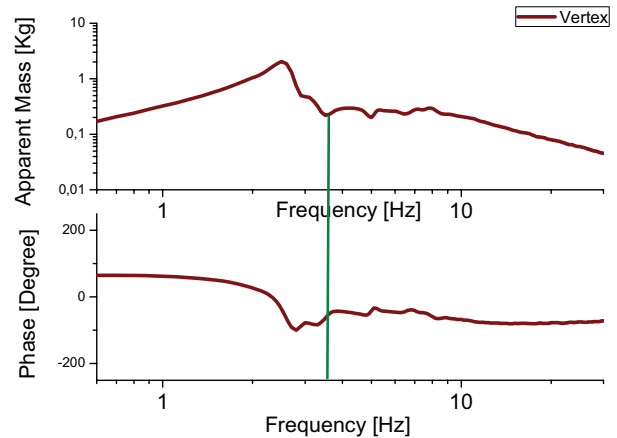


Figure 10. Transfer function in terms of apparent mass at head neck level (rotational impact).

Validation

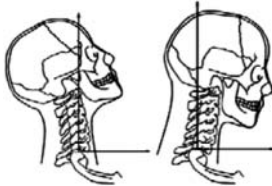

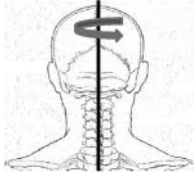
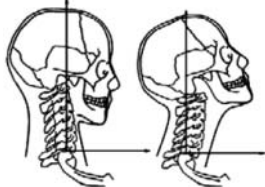

That validation [34] is the last step to be confident in the biofidelity of the FEM of the head/neck system. The validation that relies on the NDBL experimental tests focuses on the non-linear behaviour of the neck. The validation in the frequency domain allows reproducing correctly the behaviour of the head/neck system at the very beginning of the impact and for very low relative displacements. Nevertheless, these complementary validations are only managing to solve the question of the kinematics of the head relatively to the first thoracic vertebrae. Thus, and in order to obtain a complete validation of the FEM of the head/neck system, it is evidently important to use the experimental tests which permitted to record the relative motion between the cervical vertebrae in a rear impact configuration. Different studies illustrated the motion of the vertebrae in a rear impact configuration [14,34,37,38]. The experimental tests from Ono *et al.* [34] are often used for neck FEM validation as has been achieved by Ejima *et al.* [15], Kitagawa *et al.* [22] and the THUMS model. Therefore, it has been decided to reproduce an experimental test at 8 km/h in relaxed conditions. The model was constrained through linear acceleration in the sagittal and vertical plane, as well as through angular displacement in the frontal plane. The rotation angles of C3 and C7 vertebrae were calculated during 200 ms. That validation is illustrated in Figures 11–13. A good agreement between numerical and experimental results can be observed.

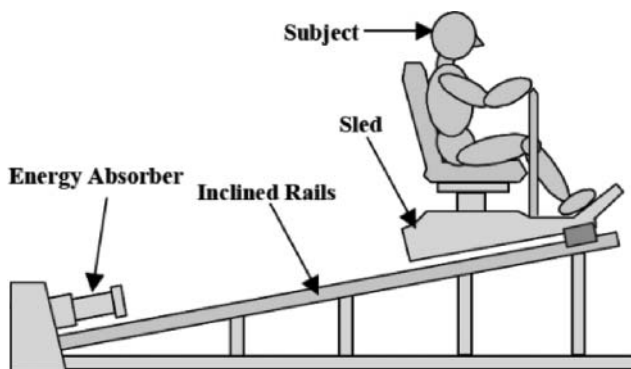
Results

Accident reconstruction

In order to reconstruct the 86 real-world accident cases with the head-neck FEM, it was necessary in a first step to simulate each case with the lumped torso model under MADYMO code. In our database, three car seat models are used. The positioning of the lumped torso model under

Table 4. Results of experimental test and simulation in terms of natural frequencies.

Mode	Mode—illustration	Average volunteer natural frequency [Hz]	Head–neck FEM natural frequency [Hz]
Flexion–extension		1.68 ± 0.2	2.8
Inclination		1.7 ± 0.2	2.6
Axial rotation		3.2 ± 0.3	3.4
S-shape		8.8 ± 0.5	11
Lateral retraction		9.5 ± 1.4	9.6

Figure 11. Test apparatus for rear impact test with volunteer subject conducted by Ono *et al.* [34].

MADYMO code was realised with the same procedure as realised by Kullgren *et al.* [25]. The head to headrest distance was therefore estimated at 69 mm for the Corolla 93 and 55 mm for the Corolla 98 and 92 mm for the Yaris. Figure 14 illustrates the positioning of the lumped torso model for the three configurations.

For each case, the pulse recording during the accident was implemented on the seat car model. The simulation times are of the order of 150–250 ms. In order to reconstruct the accidents with the head–neck FEM, the six accelerations (three linear and three angular) were extracted from MADYMO model at the first thoracic vertebrae and at the centre of gravity of the headrest. Concerning the FE simulation, the headrest rigidity was adjusted in order to

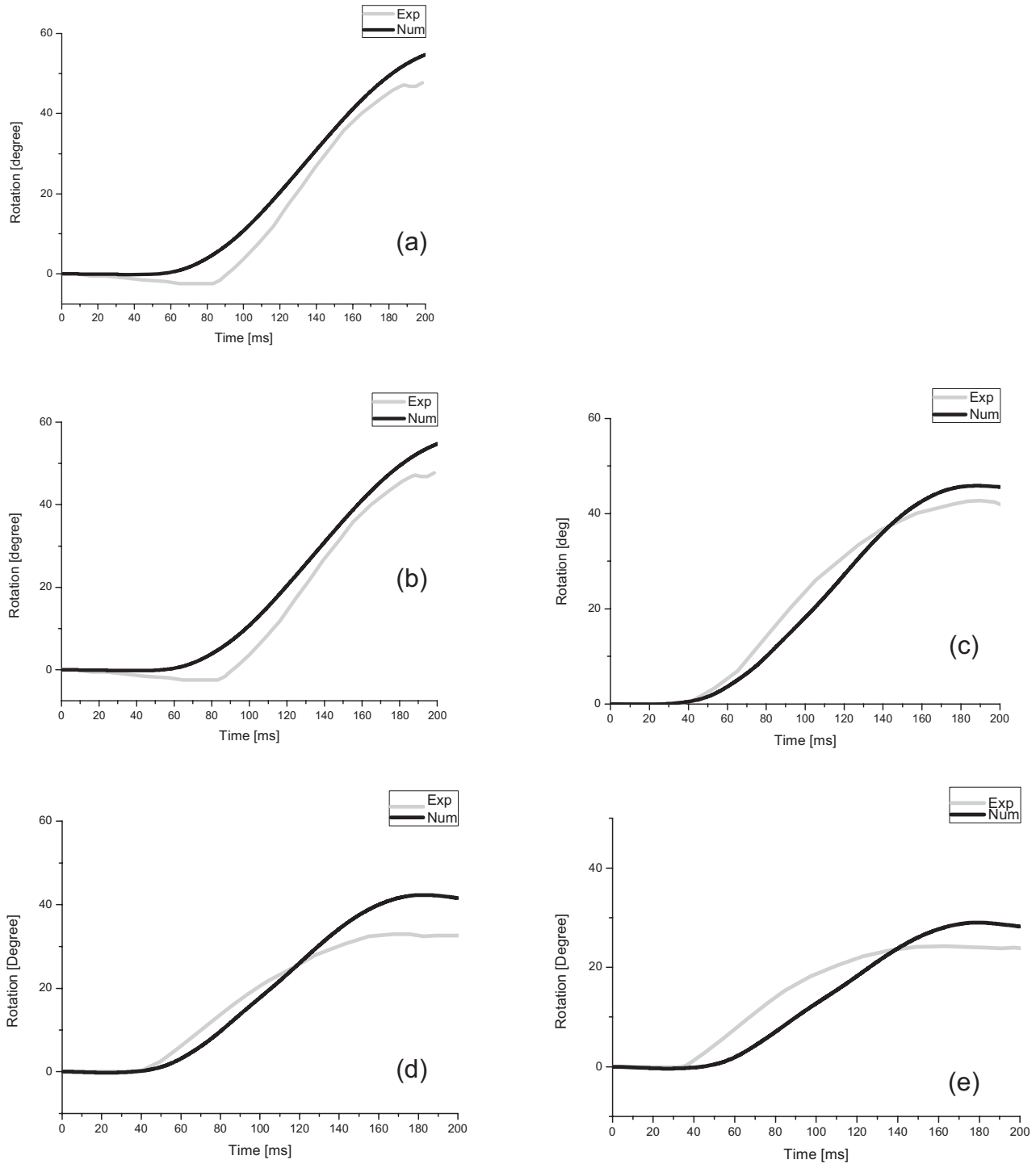


Figure 12. Comparison of head (a) and vertebral rotations [C3 (b); C4 (c); C5 (d); C6 (e)] between Uds-Head-Neck FEM and volunteer.

reproduce numerically under RADIOSS code the same impact force as those calculated with the MADYMO model. The headrest inclination and the distance were also taken into account in the FEM.

Reconstruction of a detailed case:

Corolla 98 29737

In order to illustrate the methodology used, one case is presented. It involves a male aged 36 years with a WAD1.

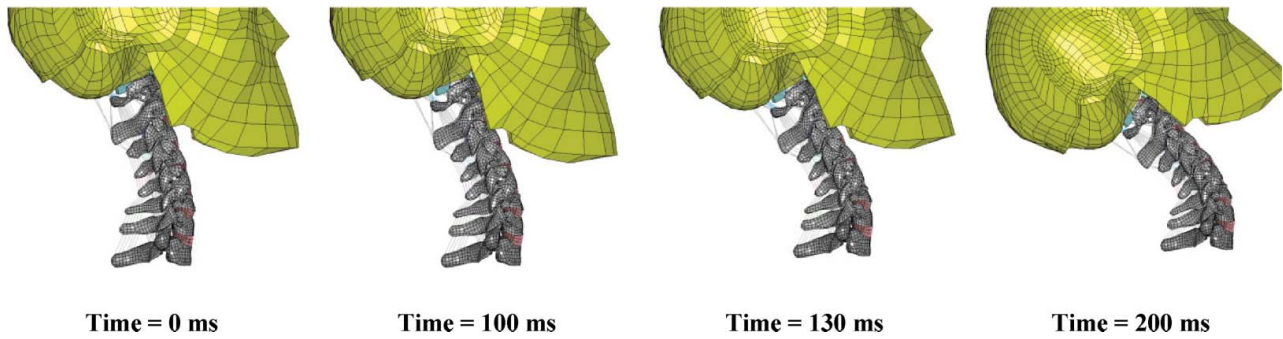


Figure 13. Kinematic response of the finite element model to a rear impact (Ono *et al.* [34]).

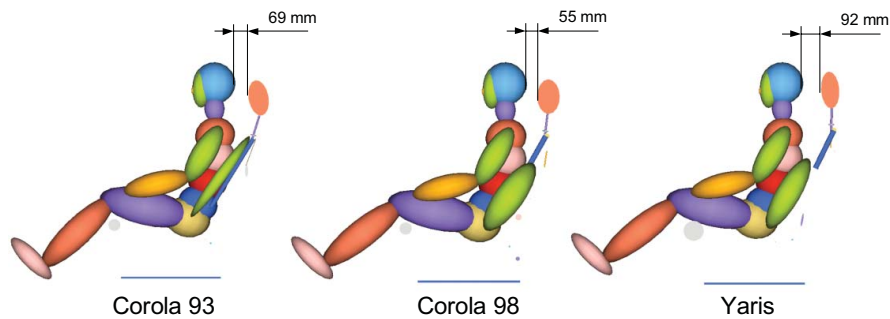


Figure 14. Position of the MC-HNT model in the three seats.

During rear impact, the cervical spine performs a complex movement composed of flexion/extension, traction/compression and shearing (Figure 15). In order to distinguish the different movements, local frames were fixed

at each facet joint and cervical vertebrae body. The local frames were oriented as follows: at the facet joint, the $+x$ direction traduced a flexion at the cervical vertebrae body, the $+x$ direction traduced the shearing and the

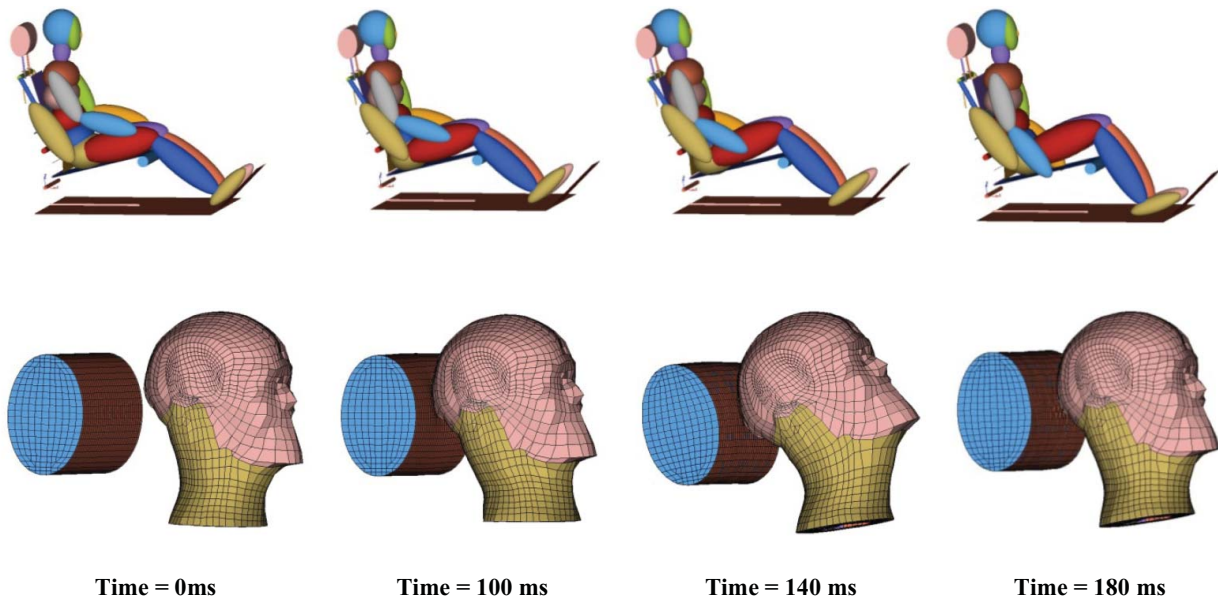


Figure 15. Kinematic response of the MADYMO model and the Head-Neck Finite element model under a rear impact (Case Corolla 98 N° 29737).

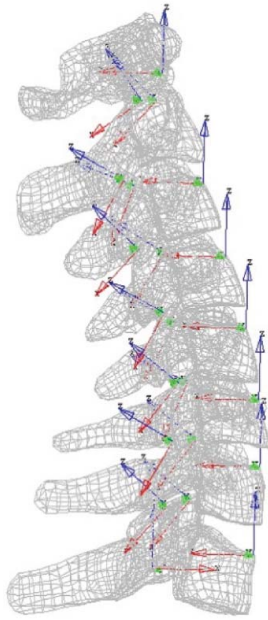


Figure 16. Local frames defined at each cervical vertebrae level.

+z direction the traction. Figure 16 illustrated the different local frames used to describe the behaviour during rear impact. Figure 17 illustrates the crash pulse recorded at the car seat and Figure 18–24 the mechanical parameters extracted with the head–neck FEM.

In this case, the average acceleration of the impact pulse is 5 g inducing a resultant acceleration of the head of 15 g (Figure 20). The head acceleration along transverse axis is null. Moreover, the angular accelerations along vertical axis and along impact direction are null too (Figure 19). This implies that movement is only in the sagittal plane.

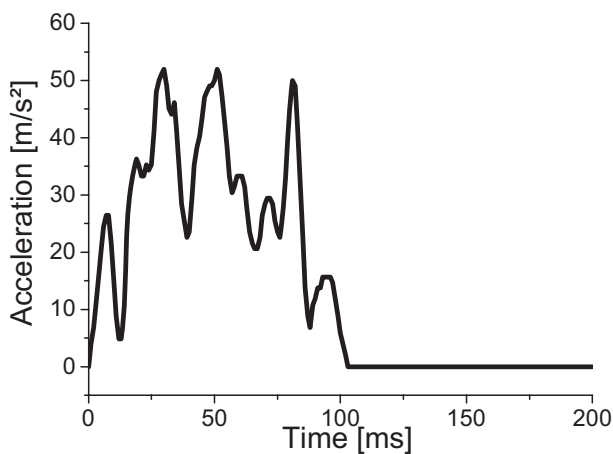
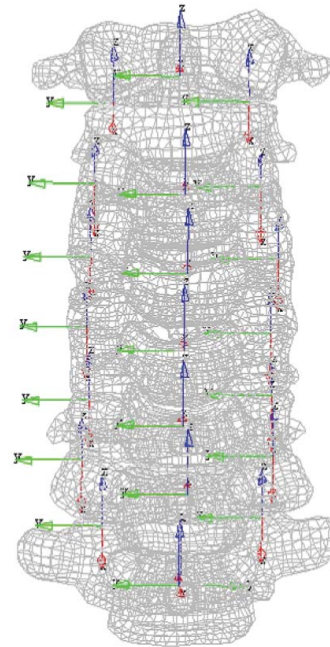


Figure 17. Acceleration recorded during the accident (case n° 29737) and applied to the seat model.



Concerning the intra-cervical motion, we can observe that the two facet joint movement is almost the same and the magnitude displacement at each level are similar (Figure 21 and 22).

Investigation of potential whiplash injury criteria

The objective of this study is to determine tolerance limits of the neck during a rear impact from injury criteria which can be associated to the degree of injury severity. In this study, the classical mechanical parameters as the linear and angular head accelerations or the NIC values are computed

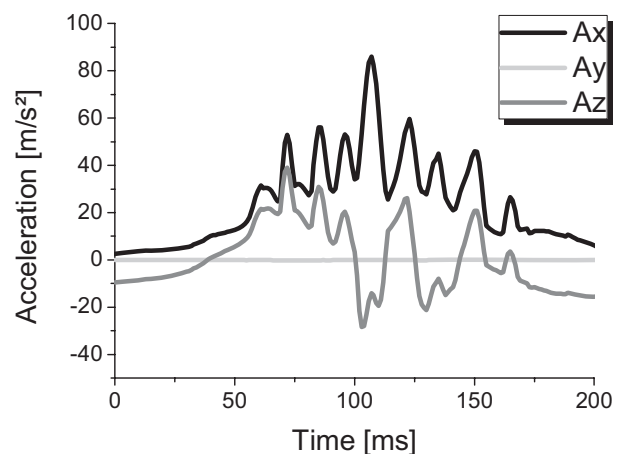


Figure 18. Linear accelerations calculated with the torso lumped model at T1.

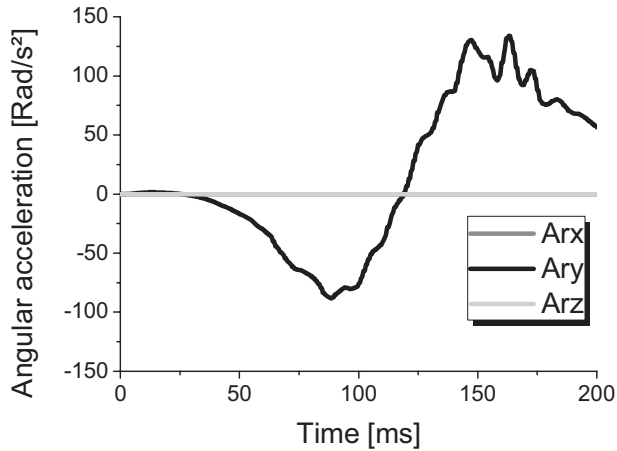


Figure 19. Angular accelerations calculated with the torso lumped model at T1.

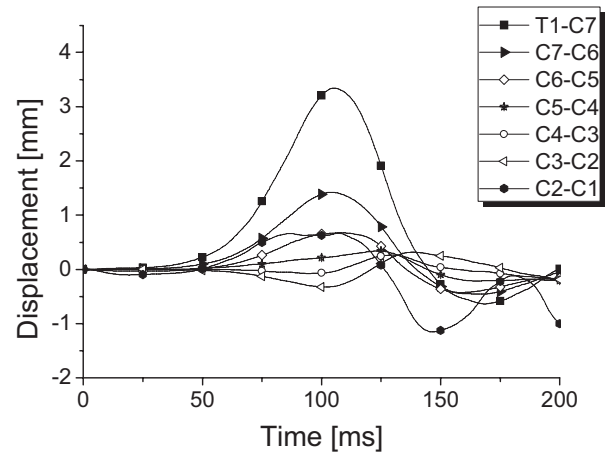


Figure 21. Relative displacement of the left facet joint in the x direction at each cervical level.

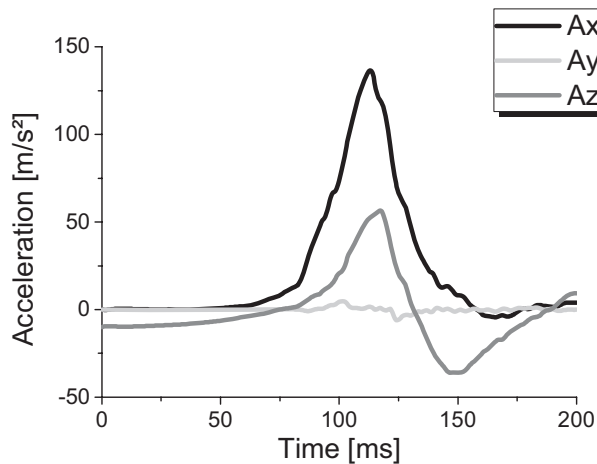


Figure 20. Linear accelerations calculated with head-neck FEM.

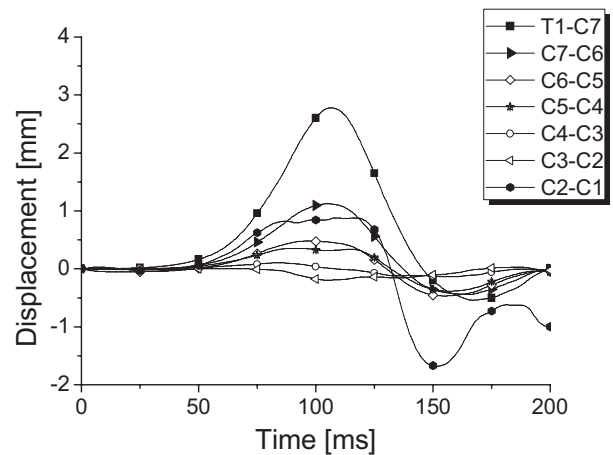


Figure 22. Relative displacement of the right facet joint in the x direction at each cervical level.

Table 5. Nagelkerke R^2 value calculated at the T1-C7 level.

R^2	Left facet joint		Right facet joint		Cervical vertebrae body			
	X direction		X direction		X direction		Z direction	
	Min	Max	Min	Max	Min	Max	Min	Max
S1	0.099	0.151	0.123	0.15	0.044	0.209	0.085	0.144
S2	0.35	0.323	0.342	0.335	0.324	0.513	0.351	0.413
S3	0.468	0.188	0.482	0.203	0.364	0.48	0.49	0.312

Table 6. Nagelkerke R^2 value calculated at the C7-C6 level.

R^2	Left facet joint		Right facet joint		Cervical vertebrae body			
	X direction		X direction		X direction		Z direction	
	Min	Max	Min	Max	Min	Max	Min	Max
S1	0.093	0.013	0.091	0.045	0.086	0.157	0.088	0.11
S2	0.356	0.06	0.366	0.079	0.381	0.361	0.373	0.251
S3	0.473	0	0.515	0	0.515	0.271	0.509	0.112

Table 7. Nagelkerke R^2 value calculated at the C6–C5 level.

R^2	Left facet joint		Right facet joint		Cervical vertebrae body			
	X direction		X direction		X direction		Z direction	
	Min	Max	Min	Max	Min	Max	Min	Max
S1	0.106	0.127	0.104	0.131	0.055	0.116	0.086	0.015
S2	0.386	0.314	0.387	0.264	0.351	0.292	0.386	0.022
S3	0.447	0.564	0.501	0.595	0.361	0.208	0.454	0.177

Table 8. Nagelkerke R^2 Value calculated at the C5–C4 level.

R^2	Left facet joint		Right facet joint		Cervical vertebrae body			
	X direction		X direction		X direction		Z direction	
	Min	Max	Min	Max	Min	Max	Min	Max
S1	0.044	0.26	0.022	0.266	0.085	0.009	0.073	0.113
S2	0.225	0.42	0.398	0.442	0.396	0.007	0.324	0.139
S3	0.221	0.57	0.458	0.684	0.473	0.097	0.372	0.221

Table 9. Nagelkerke R^2 value calculated at the C4–C3 level.

R^2	Left facet joint		Right facet joint		Cervical vertebrae body			
	X direction		X direction		X direction		Z direction	
	Min	Max	Min	Max	Min	Max	Min	Max
S1	0.074	0.218	0.064	0.16	0.059	0.136	0.059	0.123
S2	0.266	0.288	0.298	0.424	0.287	0.141	0.257	0.139
S3	0.303	0.461	0.355	0.478	0.345	0.169	0.296	0.155

in order to evaluate their level of correlation with the degree of injury. It must be noticed that in the accident database, only the severity of the injury is notified. It induces that the injury parameter cannot be localised in a specific neck area. However, it is important in contrast to conventional criteria to take into account the intra-cervical behaviour. Ono

et al. [34] highlights that shearing at a different cervical level can be an injury mechanism. Therefore, the relative displacement at each level is calculated at each cervical vertebra. The relative displacement is calculated at the two facets joint and at the cervical vertebrae body in order to distinguish the traction/compression and the shearing

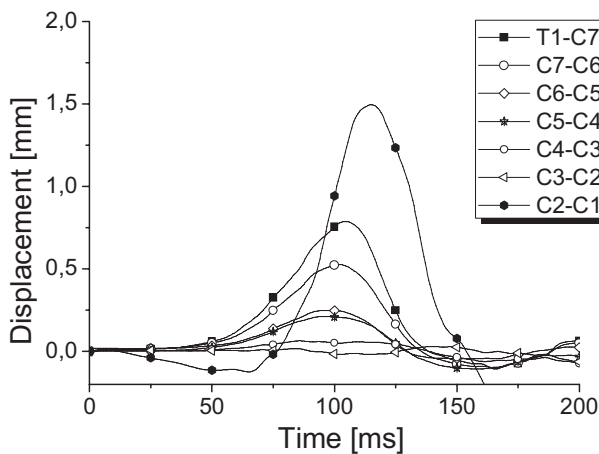


Figure 23. Relative displacement of the cervical vertebrae body in the x direction at each cervical level.

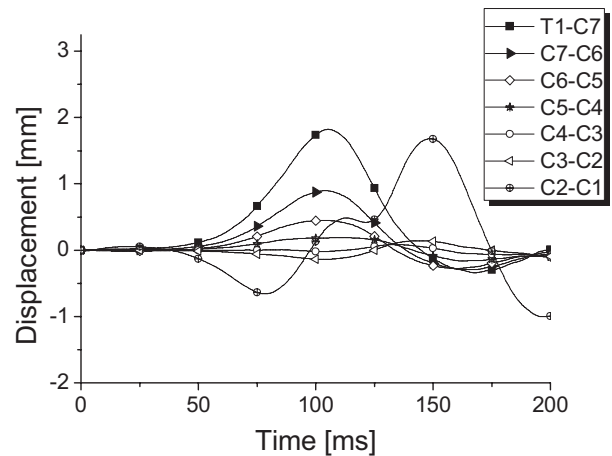


Figure 24. Relative displacement of the cervical vertebrae body in the z direction at each cervical level.

Table 10. Nagelkerke R^2 value calculated at the C3–C2 level.

R^2	Left facet joint		Right facet joint		Cervical vertebrae body			
	X direction		X direction		X direction		Z direction	
	Min	Max	Min	Max	Min	Max	Min	Max
S1	0.059	0.174	0.053	0.11	0.057	0.094	0.045	0.09
S2	0.217	0.173	0.278	0.292	0.243	0.056	0.207	0.022
S3	0.242	0.472	0.31	0.291	0.279	0.043	0.239	0.111

Table 11. Nagelkerke R^2 value calculated at the C2–C1 level.

R^2	Left facet joint		Right facet joint		Cervical vertebrae body			
	X direction		X direction		X direction		Z direction	
	Min	Max	Min	Max	Min	Max	Min	Max
S1	0.118	0.024	0.085	0.069	0.081	0.198	0.	0.149
S2	0.236	0.126	0.12	0.068	0.003	0.524	0.009	0.392
S3	0.327	0.207	0.157	0.421	0	0.706	0.032	0.54

component. Injury correlation was evaluated by calculating the correlation coefficient of logistic regression for each mechanical candidate parameter (Table 5–11). The correlation coefficient R^2 proposed by Nagelkerke [31] was used. This coefficient permits it to evaluate the quality of the regression. For that, a sample $(x_i, y_i)_{i=1, \dots, N}$ was introduced, where the x_i are the observed values of the explicative variable x and y_i are the random variables of y taking 0 for no injured and 1 for injured at case i . The logistic regression model used is a logistic function written in equation (1) which defines the probability of injury for various x . For each parameter, three logistic regressions are calculated corresponding to the risk of WAD1, the risk WAD2 and the risk of WAD3 Table 12.

It can be noticed that many criteria (values in bold (Table 5–11), $R^2_{S3} > 0.4$) can pretend to be an injury criterion with elevated correlation values. But it appears difficult to say which mechanical value correlates to the level of injury. It could be the displacement of the articular joints at the level C6-C7, or the shear at the level C5-C6. Also, the injury is never given at a precise level. It is always given as a global symptom such as ‘neck pain’ – ‘mobility restraint’. This is why the injury criterion should not be seen as a given

Table 12. Nagelkerke R^2 value calculated for the linear and angular acceleration of the Head CG. R^2 Value calculated for the NIC value.

	Head acceleration	Head angular acceleration	NIC
R^2_{S1}	0.119	0.139	0.017
R^2_{S2}	0.278	0.344	0.073
R^2_{S3}	0.252	0.332	0.12

abnormal value at a precise anatomical location, but more as a consequence of a global non-physiological movement of the cervical spine. The movement which seems for different authors to be associated with injury is the ‘s-shape’ movement of the cervical spine. Experiments made on cadavers or volunteers show that the cervical spine follows at first an ‘s-shape’ movement followed by the classical ‘flexion–extension’ movement of the cervical spine. Our study on 86 cases confirms this behaviour. Only the low-velocity cases do not show the ‘s-shape’ movement. It can therefore be concluded that the shearing mechanism at different levels of the cervical spine may be at the origin of the injuries. This criterion can be seen as the sum of the displacements of the cervical bodies along a horizontal direction (Figure 25). Depending on the intensity of the impact and on the cervical spine body level, this displacement can follow the direction of the impact or its opposite direction. To take these different displacements into account, it

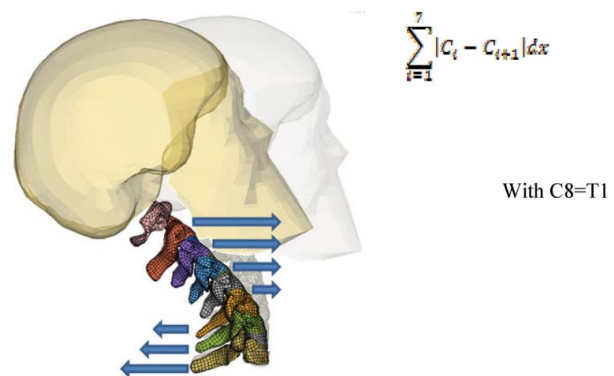


Figure 25. Illustration of the shearing in the cervical spine produce by a rear impact.

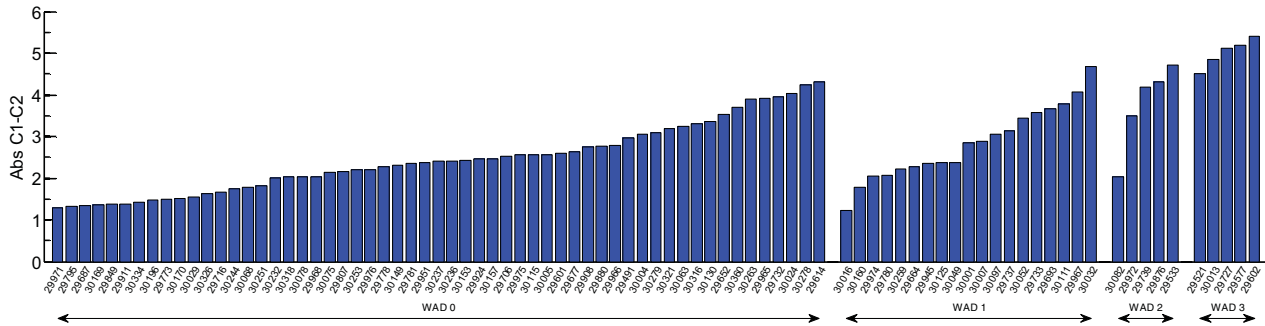


Figure 26. Representation of the mechanical parameter propose (sum of the shearing displacement at each level) versus Whiplash Associated Disorder.

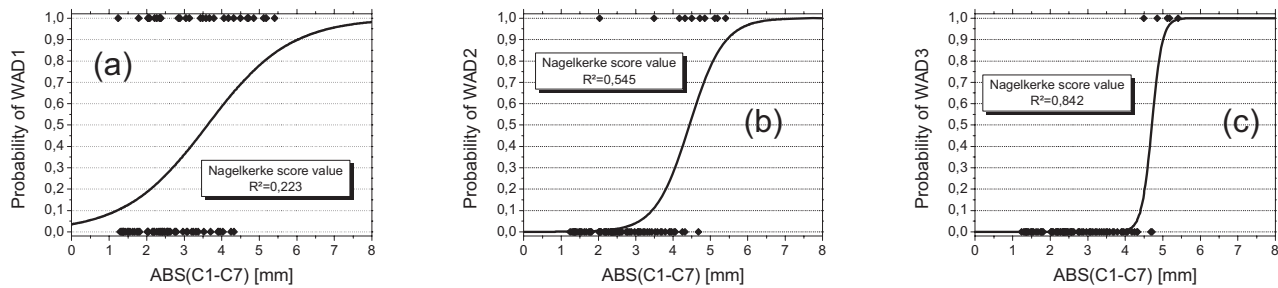


Figure 27. Risk curves of the injury criteria propose for the WAD1 (a), WAD2 (b) and WAD3 (c). R^2 WAD1 = 0.223; R^2 WAD2 = 0.545; R^2 WAD3 = 0.842.

is necessary to work with the absolute value of the displacement at each level and then to sum the displacements. The histogram in Figure 26 illustrates the correlation between the candidate mechanical parameter proposed (Shearing at each cervical level) computed with the head–neck FEM Figure 27.

Discussion

Before discussing neck injury criteria, it should be noticed that limitation of this study remains at the accident reconstruction level even if the used database is probably one of the most relevant currently available.

The car occupants are supposed to be in a standard position and to have similar mass and geometry. In addition, no detailed injury description is available as it is often not possible to identify the location of a ‘neck pain’.

Moreover, the database include a limited number of WAD2 and 3 and should be extended in order to consolidate the statistical correlation analysis. Coming to the attempt to derive neck injury criteria, it is interesting to comment on the quality of the logistical regression provided by the different candidate parameters. The initial ambition was to identify a key local intra-cervical parameter which would strongly correlate with the occurrence of injury but results show that it is finally a more global ‘cumulative’ metric which presents the highest correlation. It is then conducted

that the injury parameter is distributed through the cervical column exactly as pain is.

Finally, some authors [3,32] discussed about the possibility that whiplash injury could be due to brain injury. When potential neck injury is addressed, it appears from this study that the computed brain loading level (with the SUFEHM) is significantly lower than available brain injury threshold determined by Deck and Willinger [11] with a maximum brain Von Mises stress less than 5% risk of moderate DAI. Therefore, further head injury investigation under whiplash should more focus on local brain stem and inner ear loading conditions.

Conclusion

In the present study, a detailed head and neck FEM was developed based on existing separate models. In deep, multi-directional validation of the coupled head–neck model was performed against kinematics data in the time domain and modal characteristics in the frequency domain. Local validation of the cervical column against vertebrae-relative motion was conducted as well.

A real-world rear-impact accident database including crash pulses of 86 accidents was then considered for the computation of the 3D acceleration at T1 level for each victim. This step was used with a previously published car seat and human torso multi-body models. The extracted

T1 kinematics was finally considered as the input of FE simulation of the head and neck response.

A number of intra-cervical local and global parameters were considered as candidate parameters for neck injury criteria by investigating the correlation of the different metrics with the occurrence of injury.

Main conclusion of this extensive real-world rear-impact accident simulation and statistic analysis is that none of the existing criteria or more local parameters (such as facet distortion) presents an acceptable correlation level. However, when a more global (or cumulative) parameter is considered, such as the summation of the shearing displacement at each level, an acceptable regression parameter was observed and it was possible to derive a tentative injury risk curve for whiplash injury based on this metric.

Acknowledgement

The authors would like to thank FOLKSAM for its collaboration, the ADSEAT (FP7-SST-2008-RTD-1) project and the PREDIT (09 MT CV 05) program for their support.

Note

1. The experimentation being non-invasive and done within normal human physiological limits (the impacts to the head being largely under tolerance limits), our methodology was conducted in accordance with the practice of the responsible governing authority as described by the *Ethics Committee of the French Centre National de Recherche Scientifique (CNRS)*.

References

- [1] B. Aldman, A. Kullgren, A. Lie, and C. Tingvall, *Crash pulse recorder (CPR)-development and evaluation of a low cost device for measuring crash pulse and delta-V in real life accidents*, Proc. of the 13th ESV Conf., Paris, Paper 91-S1-W-26, 1991, pp. 188–192.
- [2] C. April and N. Bogduk, *The prevalence of cervical zygapophyseal joint pain: a first approximation*, Spine 17 (1992), pp. 744–747.
- [3] R. Boniver, *Whiplash effects on hypothalamus and the sympathetic system*, in *Whiplash Injuries. Diagnosis and Treatment*, Springer, 1996, pp. 59–63.
- [4] O. Boström, M. Krafft, B. Aldman, A. Eichberger, R. Fredriksson, Y. Haland, P. Lövsund, H. Steffan, M. Svensson, and C. Tingval, *Prediction of neck injuries in rear impacts based on accident data and simulation*, Proc. International Conference on the Biomechanics of Impacts, IRCOBI, Bron, 1997, pp. 251–264.
- [5] N. Bourdet and R. Willinger, *Human neck characterization under thoracic vibration – inter-individual and gender influence*, Proc. International Conference on the Biomechanics of Impacts, IRCOBI, Prague, 2005, pp. 257–267.
- [6] N. Bourdet and R. Willinger, *Modeling of car seat and human body interaction under rear impact*, Int. J. of Crashworthiness. 11(6) (2006), pp. 553–560.
- [7] D.L. Camacho, R.W. Nightingale, J.J. Robinette, S.K. Vanguri, D.J. Coates, and B.S. Myers, *Experimental flexibility measurements for the development of a computational head-neck model validated for near-vertex fead impact*, Proc. 41st Stapp Car Crash Conference, pp. 473–486. Society of Automotive Engineers, Warrendale, PA, 1997, Paper 973345.
- [8] A. Chawla, S. Mukherjee, and B. Karthikeyan, *Characterization of human passive muscles for impacts loads using genetic algorithm and inverse finite element methods*, J. Biomech. Modeling in Mechanobiol. 8(3) (2009), pp. 195–208.
- [9] J. Chazal, A. Tanguy, M. Bourges, G. Gaurel, G. Escande, M. Guillot, and G. Vanneville, *Biomechanical properties of spinal ligaments and a histological study of the supraspinal ligament in traction*, J. Biomech. 18(3) (1985), pp. 167–176.
- [10] S.J. Davis, L.M. Teresi, W.G. Bradley Jr, M.A. Ziemba, and A.E. Bloze, *Cervical spine hyperextension injuries: MR findings*, Radiology 180 (1991), pp. 245–251.
- [11] C. Deck and R. Willinger, *Improved head injury criteria based on head FE model*, Int. J. Crashworthiness 13(6) (2008), pp. 667–679.
- [12] M. De Jager, A. Sauren, J. Thunnissen, and J. Wismans, *A global and a detailed mathematical model for head-neck dynamics*, Proc. 40th Stapp Car Crash Conference, pp. 269–281. Society of Automotive Engineers, Warrendale, PA, 1996, Paper 962430.
- [13] Y.-C. Deng and W. Goldsmith, *Response of a human head/neck/upper-torso replica to dynamic loading-II. Analytical/numerical model*, J. Biomech. 20(5) (1987) pp. 487–497.
- [14] B. Deng, P. Begeman, K. Yang, S. Tashman, and A. King, *Kinematics of human cadaver cervical spine during low speed rear-end impacts*, Stapp Car Crash J. 44 (2000) pp. 171–188.
- [15] S. Ejima, K. Ono, K. Kaneoka, and M. Fukushima, *Development and validation of the human neck muscle model under impact loading*, Proc. International Conference on the Biomechanics of Impacts, IRCOBI, Prague, 2005, pp. 245–255.
- [16] C. Ewing, D. Thomas, L. Lustick, W. Muzzy, III, G. Willems, and P. Majewski, *Dynamic response of the human head and neck to +Gy impact acceleration*, Proc. 21st Stapp Car Crash Conference, pp. 549–586. Society of Automotive Engineers, Warrendale, PA, 1977, Paper 770928.
- [17] C. Ewing, D. Thomas, L. Patrick, G. Beeler, and M. Smith, *Dynamic response of the head and neck of the living human to -Gx impact acceleration*, Proc. 12th Stapp Car Crash Conference, pp. 424–439. Society of Automotive Engineers, Warrendale, PA, 1968, Paper 680792.
- [18] H. Ferner and J. Staubesand, *Atlas d'anatomie humaine – tête, cou, membre thoracique. Edition Médicales internationales*, Paris, 1985.
- [19] K. Gunzel, F. Meyer, N. Bourdet, and R. Willinger, *Multi-directional modal analysis of the head-neck system and model evaluation*, Proc. International Conference on the Biomechanics of Impacts, IRCOBI, York, 2009, pp. 419–422.
- [20] P.H. Halldin, K. Brolin, S. Kleiven, and H. Von Holst, *Investigation of conditions that affect neck compression-flexion injuries using numerical techniques*, Proc. 44st Stapp Car Crash Society of Automotive Engineers, 44, 2000, pp. 127–138.
- [21] F. Heitplatz, R. Sferco, P. Fay, J. Reim, A. Kim, and P. Prasad, *An evaluation of existing and proposed injury criteria with various dummies to determine their ability to predict the level of soft tissue neck injury seen in real world accidents*, 18th Technical Conference on the Enhanced Safety of Vehicles, Nagoya, Japan, 2003, pp. 1–7.
- [22] Y. Kitagawa, T. Yasuki, and J. Hasegawa, *A study of cervical spine kinematics and joint capsule strain in rear impacts*

- using a human FE model, Proc. 50th Stapp Car Crash Conf. Paper 2006-22-0020, 2006, pp. 545-566.
- [23] S. Kitazaki, *Application of experimental modal analysis to the human whole-bodyvibration*, Proceedings of the United Kingdom Informal Group Meeting on Human Response to Vibration, held at The University of Southampton, Southampton, Hampshire, 28-30 September, 1992, pp. 17-39.
- [24] A. Kullgren, A. Lie, and C. Tingvall, *Crash Pulse Recorder (CPR)-validation in full scale crash tests*, Accid. Anal. Prev. 27 (1995), pp. 717-727.
- [25] A. Kullgren, L. Eriksson, O. Boström, and M. Krafft, *Validation of neck injury criteria using reconstructed real-life rear-end crashes with recorded crash pulses*, Proc. of the 18th Techn. Conf. on ESV, Paper No. 344, Tokyo, 2003.
- [26] I.H. Lee, H.Y. Choi, J.H. Lee, and D.C. Han, *Development of finite element human neck model for vehicle safety simulation*, Int. J. Automot. Technol. 5(1) (2004), pp. 33-46.
- [27] S. Lord, L. Barnsley, and N. Bogduk, *Cervical Zygapophysal joint pain in whiplash*, in *Cervical Flexion-Extension Whiplash Injuries. Spine: State of the Art Reviews*, Vol. 12, G.A. Malanga, ed., Hanley and Belfus, Philadelphia, PA, 1993, pp. 355-372.
- [28] T. Matsushita, T.B. Sato, K. Hirabayashi, S. Fujimura, T. Asazuma, and T. Takatori, *X ray study of the human neck motion due to head inertia loading*, Proceeding of the 38th Stapp Car Crash Conference, Society of Automotive Engineers, Fort Lauderdale, FL, 1994, pp. 55-64.
- [29] J.H. Mc Elhaney, V.L. Roberts, and J.F. Hilyard, *Handbook of Human Tolerance*, Japan Automobile Research Institute, Inc. JARI, Tokyo, 1976.
- [30] F. Meyer, N. Bourdet, C. Deck, R. Willinger, and J.S. Raul, *Human neck finite element model development and validation against original experimental data*, Proc. 48th Stapp Car Crash Conf., Paper 2004-22-0008, 2004, pp. 177-206.
- [31] N.J.D. Nagelkerke, *A note on a general definition of the coefficient of determination*, Biometrika 78(3) (1991), pp. 691-692.
- [32] L.M. Odkvist, *Whiplash effects on the Vestibulo-oculomotor System*, in *Whiplash Injuries. Diagnosis and Treatment*, Springer, 1996, pp. 64-71.
- [33] K. Ono and K. Kaneoka, *Motion analysis of human cervical vertebrae during low speed rear impacts by the simulated sled*, Proc. International Conference on the Biomechanics of Impacts, IRCOBI, Hannover, 1997, pp. 223-237.
- [34] K. Ono, K. Kaneoka, A. Wittek, and J. Kajzer, *Cervical injury mechanism based on the analysis of human cervical vertebral motion and head-neck-torso kinematics during low speed rear impacts*, Proceedings of the 41st Stapp Car Crash Conference Proceedings, 1997, SAE Paper 973340, pp. 339-356.
- [35] K. Ono, S. Ejima, K. Yamazaki, F. Sato, J.A. Pramudita, K. Kaneoka, and S. Ujihashi, *Evaluation criteria for the reduction of minor neck injuries during rear-end impacts based on human FE model simulations*, Proc. International Conference on the Biomechanics of Impacts, IRCOBI, York, 2009, pp. 381-398.
- [36] M.M. Panjabi, J. Cholewicki, K. Nibu, J.N. Grauer, B.B. Babat Lawrence, and J. Dvorak, *Mechanism of whiplash injury*, Clin. Biomech. 13 (1998), pp. 239-249.
- [37] M.M. Panjabi, S. Ito, P.C. Ivancic, and W. Rubin, *Evaluation of the intervertebral neck injury criterion using simulated rear impacts*, J. Biomech. 38 (2005), pp. 1694-1701.
- [38] J.A. Pramudita, K. Ono, S. Ejima, K. Kaneoka, I. Shiina, and S. Ujihashi, *Head/neck/torso behavior and cervical vertebral motion of human volunteers during low speed rear impact: mini-sled tests with mass production car seat*, Proc. of International IRCOBI Conference, Goeteborg, 1998, pp. 201-217.
- [39] K. Schmitt, M. Muser, F. Walz, and P. Niederer, *Nkm - a proposal of for a neck protection criterion for low-speed rear-end impacts*, Traffic Inj. Prev. 3(2) (2002), pp. 117-126.
- [40] T. Sugimoto, and K. Yamazaki, *First result from the JAMA human body model project*, 19th International Technical Conference on the Enhanced Safety Vehicles, Washington, DC, 2005.
- [41] S. Sundararajan, P. Prasad, C.K. Demetropolous, S. Tashman, P.C. Begeman, K.H. Yang, and A.I. King, *Effect of head-neck position on cervical facet stretch of post mortem human subjects during low speed rear end impacts*, Stapp. Car Crash J. 48 (2004), pp. 331-372.
- [42] D.C. Viano and J. Davidsson, *Neck displacement of volunteers, BioRID P3 and Hybrid III in rear impacts: Implications to whiplash assessment by a neck displacement criterion (NDC)*, Traffic Inj. Prev. 3(2) (2002), pp. 105-116.
- [43] R. Willinger, L. Taleb, and P. Pradoura, *Head biomechanics from the finite element model to the physical model*, Proceed. IRCOBI, Brunnen, 1995, pp. 245-260.
- [44] B. Winkelstein, R. Nightingale, W. Richardson, and B. Myers, *Cervical facet joint mechanics: its application to whiplash injury*, Proc. 43rd Stapp Car Crash Conference. 1999, pp. 243-265.
- [45] J.M. Winters, *Hill-based muscle models: A systems engineering perspective*, in *Multiple Muscle Systems: Biomechanics and Movement Organization*, J.M. Winters and S.L.-Y. Woo, eds., Springer-Verlag, 1990.
- [46] J.L. Wood, *Dynamical response of human cranial bone*, J. Biomech. 4 (1971), pp. 1-12.
- [47] K. Yang, F. Zhu, F. Luan, L. Zhao, and P. Begeman, *Development of a finite element model of the human neck*, Proc. 42th Stapp Car Crash Conference, 1998, pp. 195-205. Society of Automotive Engineers, Warrendale, PA, Paper 983157.
- [48] N. Yoganadan and F.A. Pinter, *Internal loading of the human cervical spine*, J. Biomech. Eng. 119 (1997), pp. 237-240.
- [49] N. Yoganadan, S. Kumarasan, and S.A. Pintar, *Biomechaics of the cervical spine part 2. cervical spine soft tissues responses and biomechanical modelling*, Clin. Biomech. 16(1) (2001), 1-27.
- [50] N. Yoganandan, F.A. Pintar, B.D. Stemper, J.F. Cusik, R.D. Rao, and T.A. Gennarelli, *Single rear impact produces lower cervical spine soft tissue injuries*, Proc. International Conference on the Biomechanics of Impacts, 2001, pp. 201-211.
- [51] C. Zhou, T.B. Kahlil, and L.J. Dragovic, *Head injury assessment of a real world crash by finite element modelling*, Proc. of the AGARD Conf., IRCOBI, Isle of Man, 1998.

Appendix 1 Material property data for head modelling.

Part	Material property	Material parameter	Value	Element type	Reference
Face	Elastic	Density	1500 Kg/m ³	Shell	[29]
		Young modulus	4.6 + 03 MPa		
		Poisson's ratio	0.05		
Cranium (Cortical)	Elastic plastic orthotropic	Density	1500 Kg/m ⁻³	Shell	[46]
		Young modulus	1.5 E+04 MPa		
		Poisson's ratio	0.21		
		Bulk modulus	6.2 E+03 MPa		
		UTS	90.0 MPa		
		UCS	145 MPa		
Cranium (Trabecular)	Elastic plastic orthotropic	Density	1500 Kg/m ⁻³	Shell	[29]
		Young modulus	4.6 E+03 MPa		
		Poisson's ratio	0.05		
		Bulk modulus	2.3 E+03 MPa		
		UTS	35.0 MPa		
		UCS	28.0 MPa		
Scalp	Elastic	Density	1200 Kg/m ³	Solid	[51]
		Young modulus	1.67 E+01 MPa		
		Poisson's ratio	0.42		
Brain	Viscous elastic	Density	1040 Kg/m ³	Solid	Khalil <i>et al.</i>
		Bulk modulus	1.125 E+03 MPa		
		Short shear mod.	4.9 E-02 MPa		
		Long shear mod.	1.62 E-02 MPa		
		Decay constant	145 /s		
CSF	Elastic	Density	1040 Kg/m ³	Solid	[43]
		Young modulus	0.12 E-01 MPa		
		Poisson's ratio	0.49		
Falx Tentorium	Elastic	Density	1140 Kg/m ³	Shell	[51]
			3.15 E+01 MPa		
			0.45		

Material property data for neck modelling.

Part	Material property	Material parameter	Value	Element type	References
Inter-vertebral discs	Elastic	Young modulus	E = 100 Mpa	Solid	–
		Poisson's ratio	$\nu = 0.3$		
Muscle Posterior	Viscous elastic	Bulk modulus	$\beta = 2500$ Mpa	Solid	[8]
		Short shear mod	$G_0 = 0.115$ Mpa		
		Long shear mod	$G_\infty = 0.086$ Kpa		
		Decay constant	$\eta = 0.0017$ /s		
Muscle Anterior	Viscous elastic	Bulk modulus	$\beta = 2500$ Mpa	Solid	
		Short shear mod	$G_0 = 0.03995$ Mpa		
		Long shear mod	$G_\infty = 0.002949$ Mpa		
		Decay constant	$\eta = 0.0017$ /s		
Cervical vertebrae	Rigid bodies	–	–	Shell	[13]
Ligaments	Tabulated law	–	–	Springs	[9,49]
Active muscle	Tabulated law				[45]

Appendix 2

Frontal impact

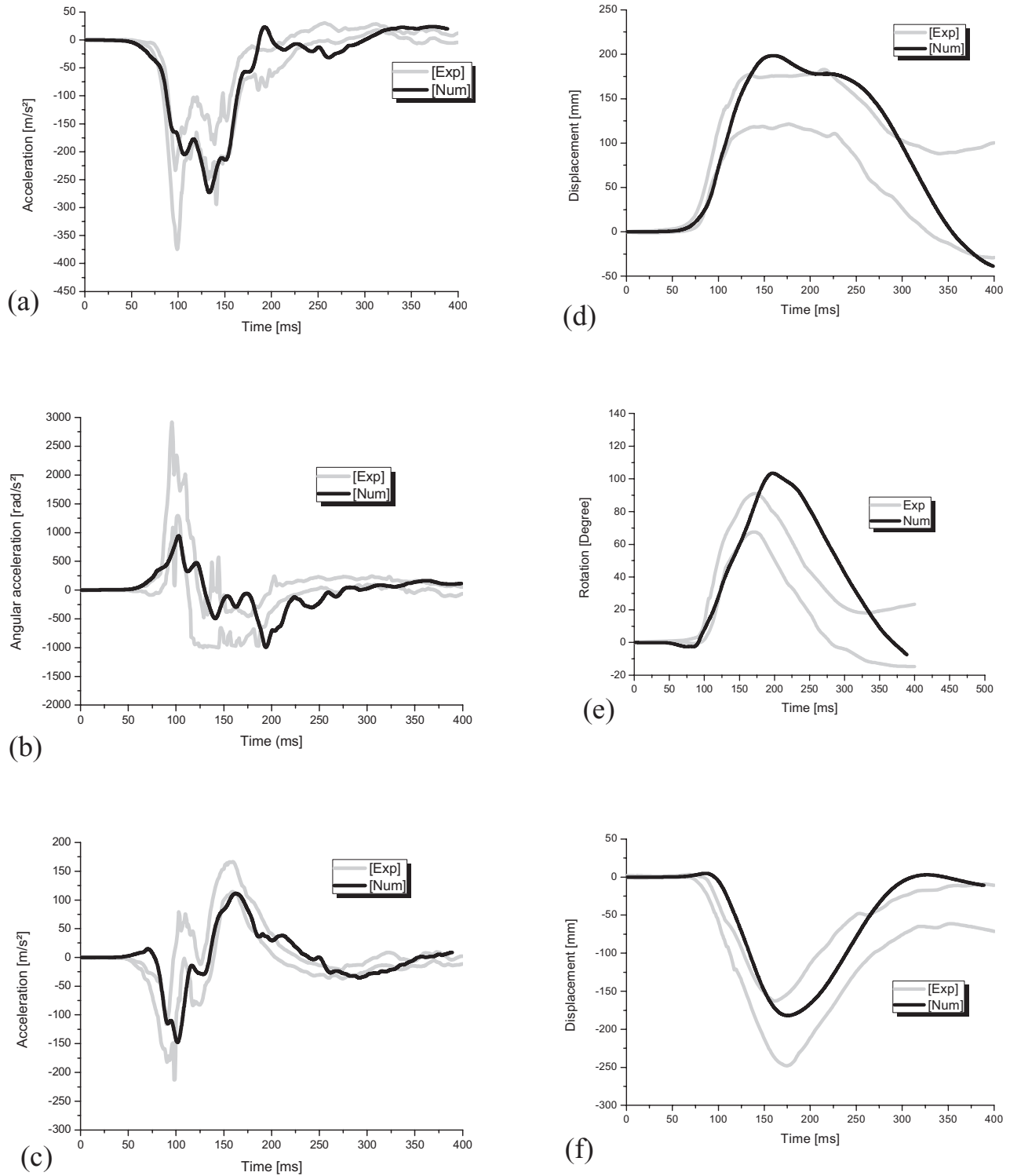


Figure A1. Numerical results for the frontal impact versus experimental corridors: (a) X-axis linear acceleration of the anatomical centre (AC) of the head, (b) Y-axis angular acceleration of AC, (c) Z-axis linear acceleration of AC, (d) X-axis displacement of AC, (e) Rotation of AC and (f) Z-axis displacement of AC.

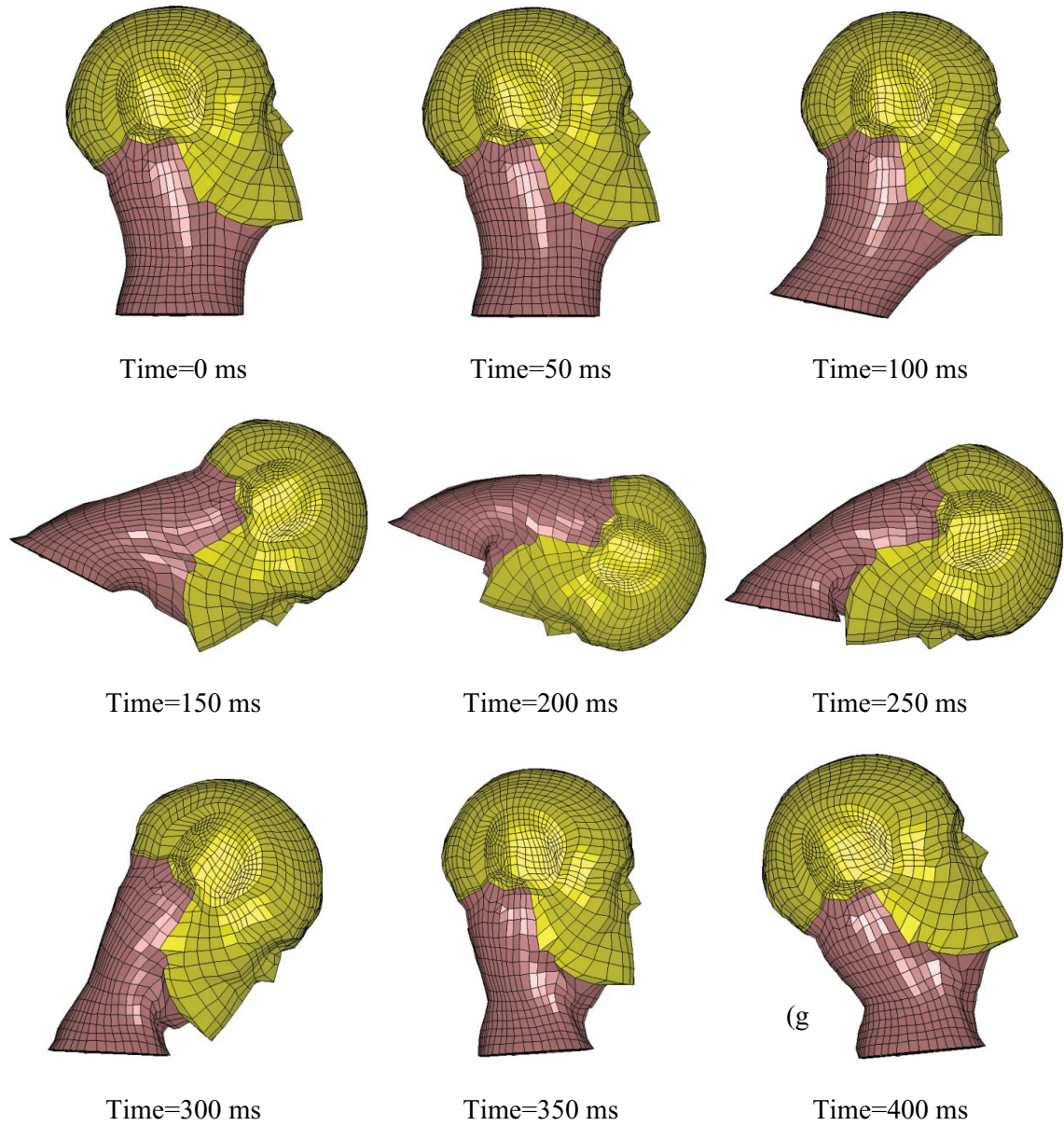


Figure A2. Kinematic response of the finite element model to a frontal impact according to NBDL [17,16].

Lateral impact

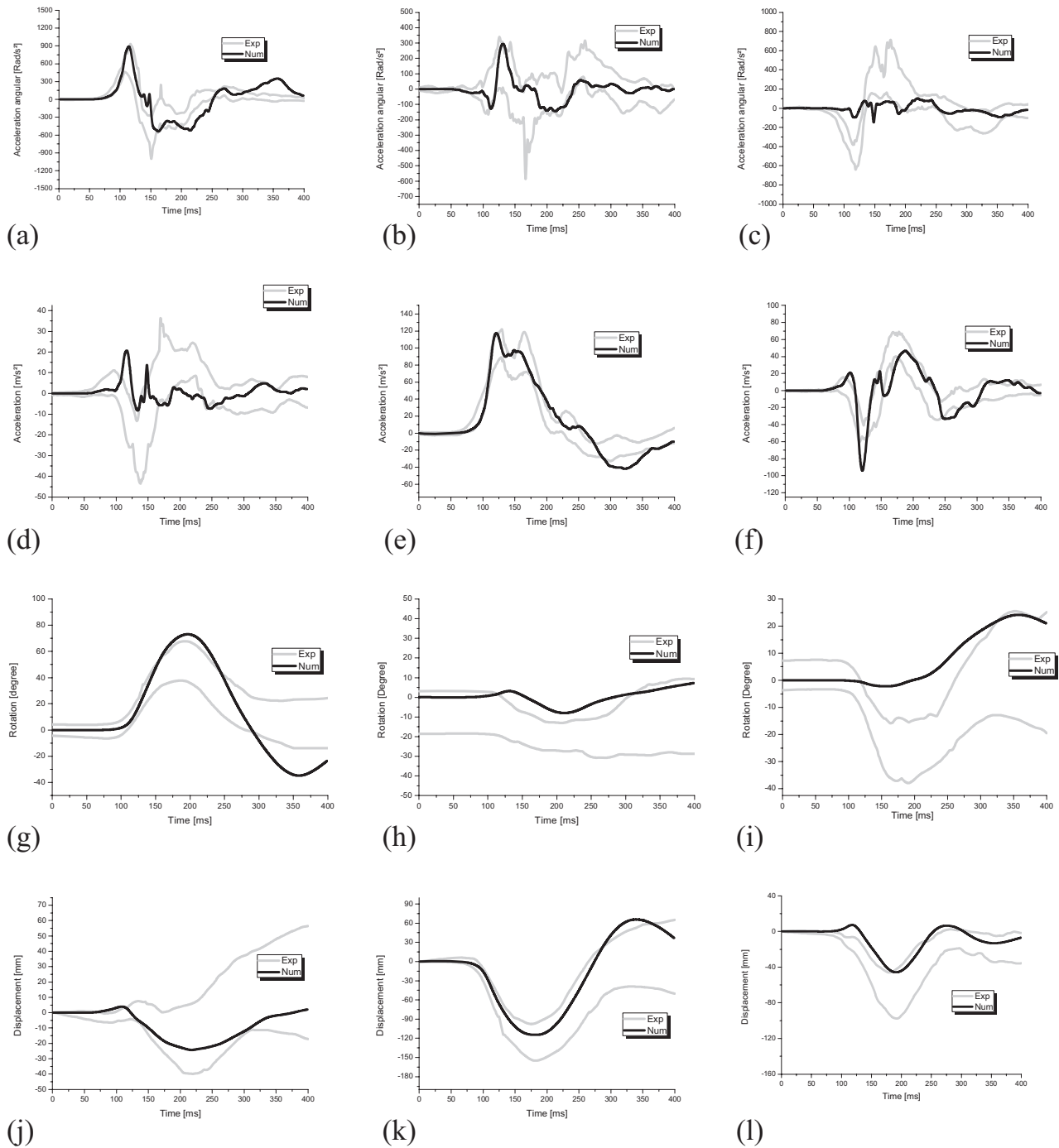


Figure A3. Numerical neck responses versus experimental corridors under lateral impact: *X*-axis (a), *Y*-axis (b) and *Z*-axis (c) angular accelerations of the anatomical centre (AC) of the head respectively, *X*-axis (d), *Y*-axis (e) and *Z*-axis (f) linear accelerations of AC respectively, *X*-axis (g), *Y*-axis (h) and *Z*-axis (i) rotation of AC respectively, *X*-axis (j), *Y*-axis (k) and *Z*-axis (l) displacement of AC respectively.

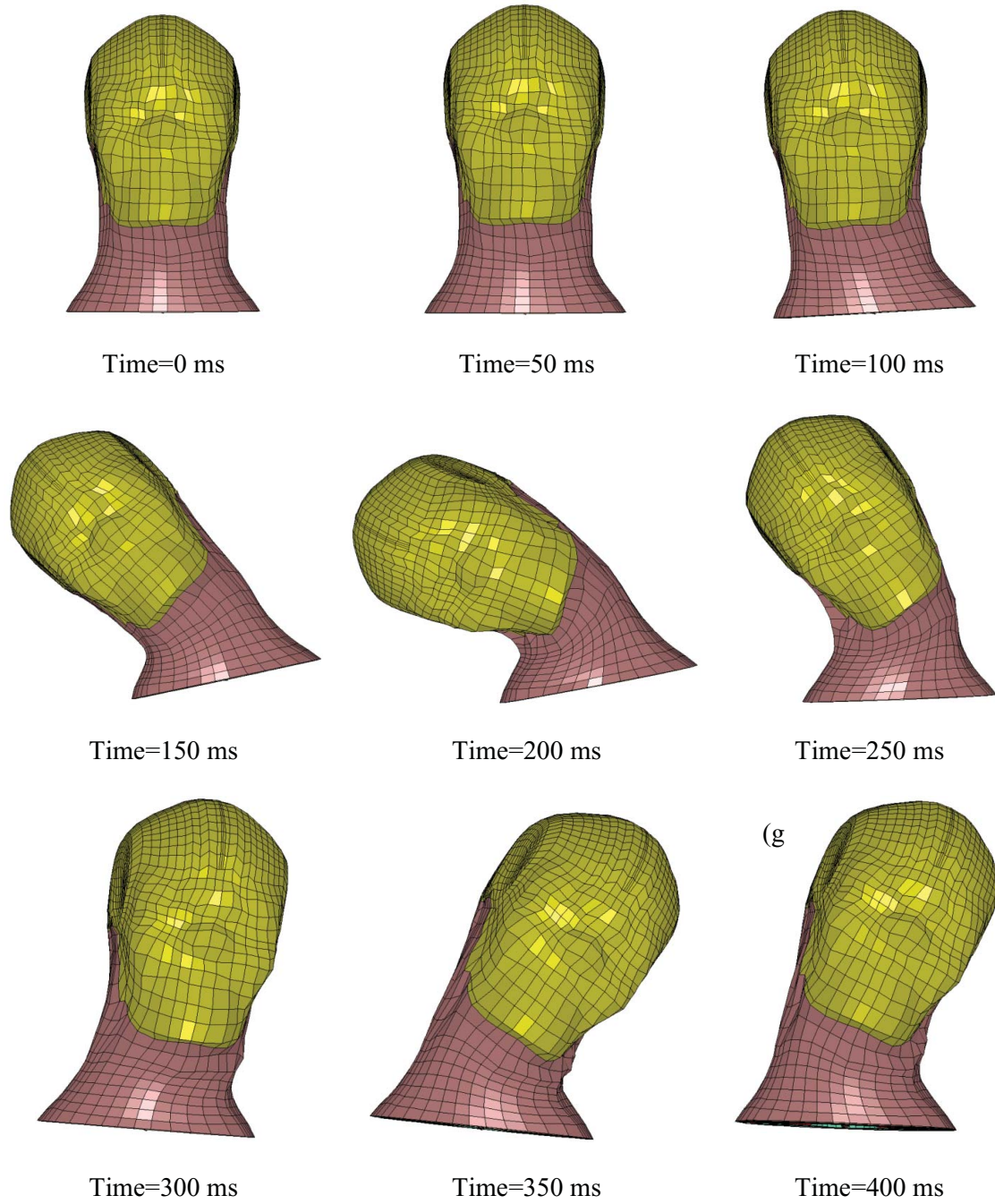


Figure A4. Kinematic response of the finite element model to a lateral impact according to NBDL [17,16].

Oblique impact

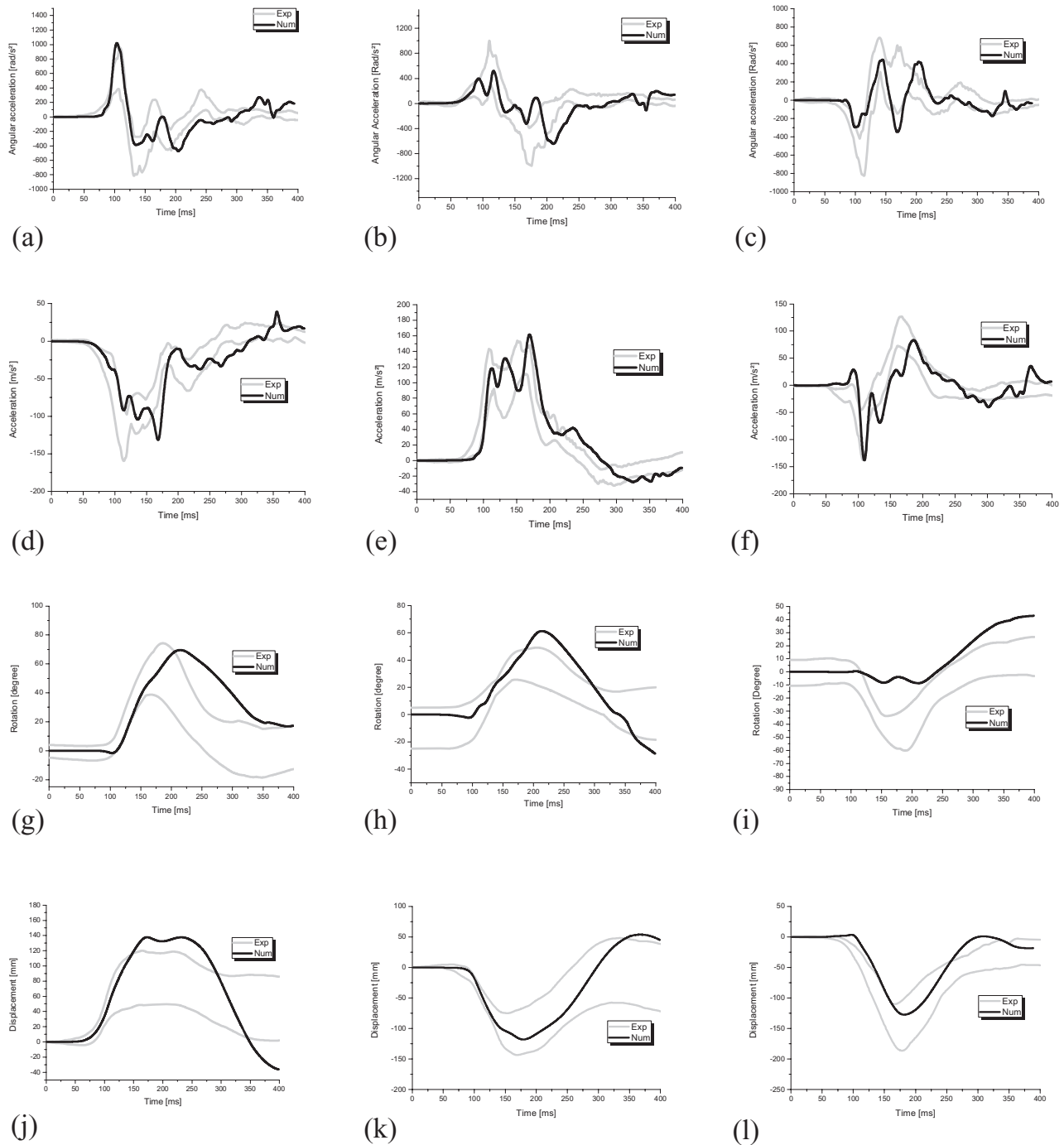


Figure A5. Numerical neck responses versus experimental corridors under oblique impact: *X*-axis (a), *Y*-axis (b) and *Z*-axis (c) angular accelerations of AC respectively, *X*-axis (d), *Y*-axis (e) and *Z*-axis (f) linear accelerations of AC respectively, *x*-axis (g), *Y*-axis (h) and *Z*-axis (i) rotation of AC respectively, *x*-axis (j), *Y*-axis (k) and *Z*-axis (l) displacement of AC respectively.

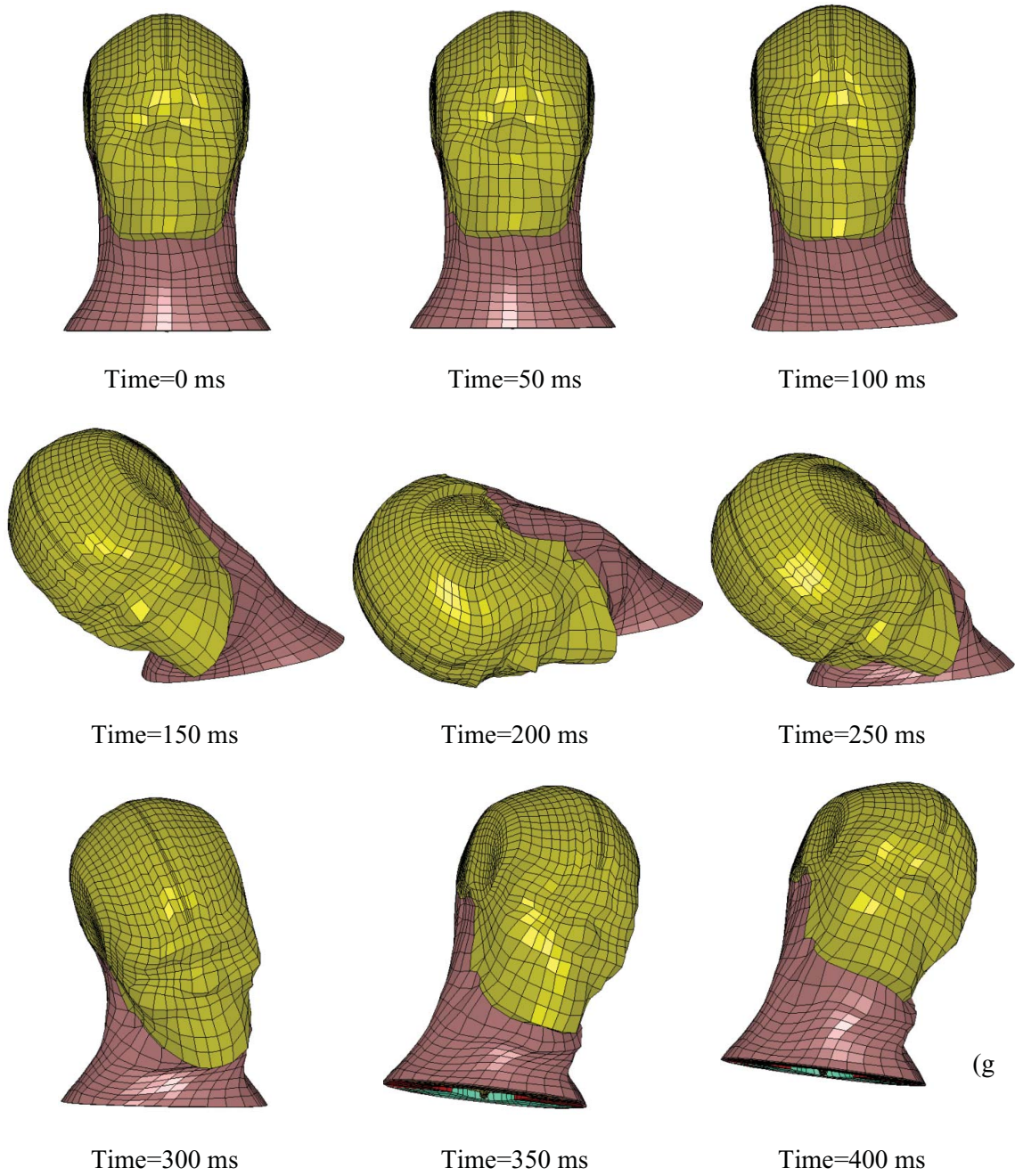


Figure A6. Kinematic response of the finite element model to an oblique impact according to NBDL [17,16].